Thesis for the degree of Doctor of Philosophy

Robust Vehicular Communications for Traffic Safety— Channel Estimation and Multiantenna Schemes

Keerthi Kumar Nagalapur

CHALMERS

Communication Systems Group
Department of Electrical Engineering
Chalmers University of Technology

Gothenburg, Sweden 2018

Robust Vehicular Communications for Traffic Safety—
Channel Estimation and Multiantenna Schemes
Keerthi Kumar Nagalapur

ISBN 978-91-7597-743-0
Doktorsavhandlingar vid Chalmers tekniska högskola
Series number: 4424
ISSN 0346-718X

This thesis has been prepared using LaTeX and Ti*k*Z/PGF.

Communication Systems Group
Department of Electrical Engineering
Chalmers University of Technology
SE-412 96 Gothenburg, Sweden

Printed by Chalmers Reproservice,
Gothenburg, Sweden, May 2018.

Abstract

Vehicular communications, where vehicles exchange information with other vehicles or entities in the road traffic environment, is expected to be a part of the future transportation system and promises to support a plethora of applications for traffic safety and efficiency. In particular, vehicle-to-vehicle (V2V) communication promises to support numerous traffic safety applications by enabling a vehicle to broadcast its current status to all the other vehicles in its surrounding.

Vehicular wireless channels can be highly time- and/or frequency-selective due to high mobility of the vehicles and/or large delay spreads. IEEE 802.11p has been specified as the physical layer standard for vehicular communications, where the pilots are densely concentrated at the beginning of a frame. As a consequence, accurate channel estimation in later parts of the frame becomes a challenging task. In this thesis, a solution to overcome the ill-suited pilot pattern is studied; a cross-layered scheme to insert complementary pilots into an 802.11p frame is proposed. The scheme does not require modifications to the 802.11p standard and a modified receiver can utilize the complementary pilots for accurate channel estimation in vehicular channels.

The metallic components of present-day vehicles pose a challenge in designing antenna systems that satisfy a minimum required directive gain in the entire horizontal plane. Multiple antennas with contrasting directive gain patterns can be used to alleviate the problems due to low directive gains. A scheme that combines the output of L antennas to the input of a single-port receiver is proposed in the thesis. The combining scheme is designed to minimize the probability of a burst error, i.e., an unsuccessful decoding of K consecutive packets from a transmitter arriving in the direction of low directive gains of the individual antennas. To minimize complexity, the scheme does not estimate or use any channel state information. It is shown using measured and simulated directive gain patterns that the probability of burst errors for packets arriving in the direction of low directive gains of the individual antenna elements can be minimized.

The enhanced distributed channel access (EDCA) scheme is used in V2V communications to facilitate the sharing of allocated time-frequency resources. The packet success ratio (PSR) of the broadcast messages in the EDCA scheme depends on the number of vehicles and the packet transmission rate. The interference at a receiving vehicle increases due to multiple simultaneous transmissions when the number of vehicles grows beyond a limit, resulting in the decrease of the PSR. A receiver setup with sector antennas, where the output of each antenna can be processed separately to decode a packet, is described in the thesis with a detailed performance analysis. A significant increase in the PSR is shown in a dense vehicular scenario by using four partially overlapping sector antennas compared with a single omnidirectional antenna setup.

Keywords: All-to-all Broadcast, Channel Estimation, Cross-layer Pilot Scheme, Multi-antenna Schemes, Sector Antennas, Traffic Safety, Vehicular Communications (V2X)

List of Publications

Included Papers

This thesis is based on the following appended papers.

[A] K. K. Nagalapur, F. Brännström, and E. G. Ström, "On channel estimation for 802.11p in highly time-varying vehicular channels," in *Proc. IEEE International Conference on Communications (ICC)*, Sydney, pp. 5659–5664, June 2014.

[B] K. K. Nagalapur, F. Brännström, E. G. Ström, F. Undi, and K. Mahler, "An 802.11p cross-layered pilot scheme for time- and frequency-varying channels and its hardware implementation," *IEEE Transactions on Vehicular Technology*, vol. 65, no. 6, pp. 3917–3928, Apr. 2016.

[C] K. K. Nagalapur, E. G. Ström, F. Brännström, J. Carlsson, and K. Karlsson, "Robust connectivity with multiple directional antennas for vehicular communications," submitted to *IEEE Transactions on Intelligent Transportation Systems*, May 2018.

[D] K. K. Nagalapur, F. Brännström, and E. G. Ström, "Performance analysis of receivers using sector antennas for broadcast vehicular communications," submitted to *IEEE Transactions on Communications*, May 2018.

Other Work

[a] K. K. Nagalapur, F. Brännström, and E. G. Ström, "Method to introduce complementing training symbols into an 802.11p OFDM frame in vehicular communications," U.S patent US9621389B2, issued on Apr. 11, 2017 (acquired by Volvo Car Corporation).

[b] K. K. Nagalapur, E. G. Ström, F. Brännström, J. Carlsson, and K. Karlsson, "A simple method for robust vehicular communication with multiple nonideal antennas," in *Proc. IEEE International Conference on Microwaves for Intelligent Mobility*, Munich, Apr. 2018.

Acknowledgments

This thesis is a result of the interaction and collaboration with several people during my PhD studies. I am grateful to everyone who has directly or indirectly contributed to the thesis.

To begin with, I sincerely thank my supervisors Prof. Fredrik Brännström and Prof. Erik Ström for their patience and guidance over the last five and a half years. Together, you have taught me the importance of understanding the broader perspective while giving importance to the details. You have always been open-minded towards my ideas and working with you has been a great learning experience that I will cherish in the years to come.

I extend my gratitude to the administration staff at the Department of Electrical Engineering for all the help over the years. I would like to thank my colleagues in the *Chase* and *ChaseOn* projects for their insights into the practical aspects of communications. Thanks to my colleagues at Fraunhofer Heinrich Hertz Institute, Berlin for hosting me. Especially, I am grateful to Fabian Undi for his patience in helping me with the aspects of hardware implementation.

My life at Chalmers as a PhD student has been much more than research and publications. I have been fortunate to be surrounded by very diverse and friendly people during my PhD studies. Thanks to all the friends and colleagues at the Department of Electrical Engineering for the amazing environment and making my PhD period an enriching experiencing. A special mention goes to my office mate during the last two years; Johan, it was fun sharing the office with you and I hope you have found a replacement for my awesome humming. I also take this opportunity to thank my friends outside the department for making the experience of living away from home a pleasant one.

Finally and most importantly, I am grateful to my parents Basavaraj and Asha for their dedication and sacrifices towards my education.

Keerthi Kumar Nagalapur
Gothenburg, May 2018

Financial Support

This research was financed by:

- Chalmers Antenna Systems Excellence Center (*Chase*), a Swedish Governmental Agency of Innovation Systems (Vinnova) excellence center, in the project 'Antenna Systems for V2X Communication'.
- *ChaseOn* in a project financed by Vinnova, Chalmers, Bluetest, Ericsson, Keysight, RISE, Smarteq, and Volvo Cars.

Thanks to European COST IC 1004 STSM and Ericsson Research Foundation grants for partially funding my visits to Fraunhofer Heinrich Hertz Institute, Berlin and IEEE International Conference on Communications 2014.

Acronyms

AC	access class
ADC	analog-to-digital converter
AGC	automatic gain control
AIFS	arbitration interframe space
AOA	angle-of-arrival
AOD	angle-of-departure
APP	a-posteriori probability
BER	bit error rate
CAM	cooperative awareness message
CDP	constructed data pilot
CP	cyclic prefix
CRC	cyclic redundancy check
CSI	channel state information
CSIT	channel state information at the transmitter
CSMA/CA	carrier-sense multiple access with collision avoidance
CTS	clear to send
DAC	digital-to-analog converter
DCF	distributed coordination function
DENM	decentralized environmental notification message
DIFS	DCF interframe space
DSP	digital signal processing

DSRC	dedicated short range communications
DTMC	discrete time Markov chain
EDCA	enhanced distributed channel access
EGC	equal gain combining
FER	frame error rate
FFT	fast Fourier transform
FPGA	field programmable gate array
GLOSA	green light optimal speed advisory
GSCM	geometry-based stochastic channel model
HDL	hardware description language
HLL	high level language
I2V	infrastructure-to-vehicle
IEEE	Institute of Electrical and Electronics Engineers
ITS	intelligent transportation systems
LLC	logical link control
LLR	log-likelihood ratio
LMMSE	linear minimum mean squared error
LNA	low noise amplifier
LO	local oscillator
LOS	line-of-sight
LPF	low pass filter
LS	least-squares
LT	long training
MAC	medium access control
MCS	modulation and coding scheme
MF	modified 802.11p frame
MIMO	multiple input multiple output
MPC	multipath component
MRC	maximal ratio combining
MSE	mean squared error
NLOS	non line-of-sight
OCB	outside the context of a basic service set

OFDM	orthogonal frequency-division multiplexing
OLOS	obstructed LOS
PA	power amplifier
PAPR	peak to average power ratio
pdf	probability distribution function
PDP	power delay profile
PHY	physical
PSR	packet success ratio
PT	pseudo training
QAM	quadrature amplitude modulation
RAM	random access memory
rms	root mean square
ROM	read only memory
RTS	request to send
RX	receiver
SC	selection combining
SF	standard 802.11p frame
SINR	signal-to-interference plus noise power ratio
SISO	single input single output
SNR	signal-to-noise power ratio
STA	spatial temporal averaging
STBC	space-time block code
TX	transmitter
TXOP	transmission opportunity
US	uncorrelated scattering
V2V	vehicle-to-vehicle
V2X	vehicle-to-everything
WSS	wide sense stationary
WSSUS	wide sense stationary uncorrelated scattering

Contents

Part I

Overview

Chapter 1

Introduction

1.1 Background

Active and passive safety features in vehicles have significantly improved the safety of passengers over the last few decades and continue to do so. Optical vision and radar based technologies have been recently adopted in vehicles to monitor the immediate surroundings, and thereby prevent collisions and warn the drivers of hazardous situations. However, radar and vision based systems are limited by small coverage distance and their inability to sense vehicles that are obstructed by other obstacles. Wireless radio communications can overcome the aforementioned limitations with their ability to support communications in non line-of-sight (NLOS) scenarios over longer distances. To further improve traffic safety and enable a wide range of applications related to traffic efficiency and fuel efficiency, wireless vehicular communications are considered for future transportation systems.

Vehicular communications, which involves communication between vehicles or the communications between a vehicle and other entities such as a road side unit, a pedestrian, etc., is collectively referred to as vehicle-to-everything (V2X) communications. V2X communications enable a variety of road traffic applications; an extensive list of a basic set of applications supported under cooperative intelligent transportation systems (ITS) can be found in [1, 2]. Intersection collision warning is an important application of vehicle-to-vehicle (V2V) communications, where a driver is warned about an impending collision with another vehicle which might be hidden to the driver's vision due to an obstacle [2]. As an example of nonsafety applications and infrastructure-to-vehicle (I2V) communications, green light optimal speed advisory (GLOSA) advises the drivers to maintain a driving speed to avoid stopping at traffic signals [2]. This application is enabled by the broadcast of status messages by traffic signals and has been shown to reduce the fuel consumption of transport vehicles [3].

Two different technologies have been explored to enable V2X communications, namely, i) direct V2X communications without a central coordinator and ii) cellular network

based V2X communications. In direct V2X communications, vehicles and roadside units communicate with each other in an ad-hoc fashion without the requirement of a central coordinator and therefore are not limited by the availability of supporting infrastructure. Whereas, in cellular network aided V2X communications, the cellular network is used to either transport the information or coordinate direct communications between vehicles; however, vehicles may be allowed to communicate without the assistance of a cellular network in specific scenarios. This thesis focuses on direct V2X communications technology that does not depend on a coordinator or a cellular network; and V2X communications in the rest of the thesis refers to direct V2X communications.

Standardization efforts have been made to bring V2X communications into practice. ITS-G5 and dedicated short range communications (DSRC) standards are specified for V2X communications in Europe and US, respectively [4, 5]. Among V2X communications, V2V communication plays an essential role in supporting the safety applications as it enables low latency intervehicular communication without requiring the support of additional infrastructure. In V2V communications, the vehicles broadcast periodic status messages and event driven messages [1]. The periodic status messages referred to as cooperative awareness messages (CAMs) contain position, heading, velocity, acceleration, and other details of the broadcasting vehicle [6]. The event driven messages referred to as decentralized environmental notification messages (DENMs) are broadcast to convey the occurrence of specific events, for example hard breaking [7]. Vehicles combine the information received from other vehicles with their own to enable applications that advise the driver and/or control the vehicle to a certain extent.

The V2X communication systems have to be designed considering the specific nature of traffic applications and vehicular environments. To understand the wireless channels in which the V2X communication systems will be deployed, several channel measurement campaigns, characterization, and modeling studies have been conducted [8–15]. The studies indicate that the vehicular channels are highly time- and frequency-selective, and traffic scenario dependent. For example, channels in a highway scenario and an urban intersection scenario have different characteristics. V2V channels are considered to be the most challenging for enabling reliable communications due to the mobile nature of both the transmitter and the receiver.

Both the ITS-G5 and DSRC standards use the physical layer specified in Institute of Electrical and Electronics Engineers (IEEE) 802.11p with a channel spacing of 10 MHz for safety applications [16]. IEEE 802.11p is an amendment to the IEEE 802.11a standard which was originally designed for static indoor environments [17]. In contrast to 802.11a, outside the context of a basic service set (OCB) operation mode has been chosen as the default operation mode in 802.11p, where authentication, association, and data confidentiality services are not used. The OCB operation mode is well suited for rapid broadcast communications spanning over short durations and traffic scenarios where vehicles are continuously changing their location. Furthermore, there is no mechanism for a receiver to acknowledge the success or failure of reception of a frame in the broadcast mode. This requires the vehicular communication systems to support reliable communications without the aid of retransmission strategies. The 802.11p specification [16] is now obsolete and the amendments proposed by it are now a part of the IEEE 802.11 specifications [17]; despite this, the vehicular communications standard based on the amendments is referred

to as 802.11p in this thesis.

Accurate channel estimates are necessary to enable reliable communications in coherent wireless communication systems. Since 802.11a was designed to operate in static indoor environments, the pilots allocated for channel estimation are densely concentrated at the beginning of a frame. The dense concentration of the pilots at the beginning of the frame and the highly time- and frequency-varying nature of the vehicular channels makes robust channel estimation at the later parts of the frame a challenging task. Modification of the pilot pattern, or the use of decision feedback or iterative channel estimation schemes to enable robust channel estimation have been proposed in the literature [18–28].

Antenna systems for V2V communications have to be designed considering the all-to-all broadcast nature of the CAMs and DENMs. Since the CAMs and DENMs are intended for all the vehicles in the transmission range, the antenna systems have to be designed to achieve omnidirectional coverage, i.e., satisfy a minimum required antenna gain in the entire horizontal/azimuth plane. The metallic roof and components of vehicles present a challenge in achieving omnidirectional coverage with a single antenna element [8]. Solutions involving multiple antenna elements have been proposed to achieve omnidirectional coverage with the added benefit of diversity gain [29–32].

The absence of a central coordinator requires the use of a medium access control (MAC) scheme to facilitate the transmitters to share the common time-frequency resources. A MAC scheme referred to as enhanced distributed channel access (EDCA) has been specified for V2X communications in both ITS-G5 and DSRC standards; it is based on the well known carrier-sense multiple access with collision avoidance (CSMA/CA) mechanism with additional features to impose different priorities on different packet types. The EDCA scheme operates without any acknowledgments or handshake signals in the broadcast scenario. The performance of the EDCA scheme has been studied in [33–35]. A common conclusion of the studies is that the packet success ratio (PSR) decreases significantly when the number of vehicles increases beyond a certain point.

1.2 Objectives

The thesis addresses some of the challenges with the V2X communications outlined above. In particular,

- to improve the channel estimation, a cross-layered pilot insertion scheme to introduce complementary pilots into the 802.11p frame using layers above the physical (PHY) and MAC layers, is presented. The proposed scheme is backward compatible with the standard 802.11p transceivers with the requirement of a software/firmware update in higher layers. The compatibility and feasibility of the proposed scheme is validated through hardware implementation and measurements.

- to provide robust connectivity when the antennas exhibit low gains in certain directions and the dominant component of a received signal arrives with a narrow angular spread, a low complexity antenna combining scheme is proposed. The combining scheme allows the use of multiple directional antennas in the case of a single-port receiver to provide robust connectivity, i.e., minimize the probability

of K consecutive packet errors for the worst-case angle-of-arrival (AOA) of the dominant component.

- a setup that uses multiple sector antennas together with a receiver that can decode several packets simultaneously is described with a detailed performance analysis. The setup is shown to provide significant improvement in PSR compared with a single omnidirectional antenna setup in the case of dense broadcast vehicular networks .

1.3 Outline

In Chapter 2, characteristics of the vehicular channels and the channel models are discussed. Chapter 3 presents the 802.11p frame format and a few channel estimation schemes studied in the literature. Also, the proposed cross-layered pilot insertion scheme is described in this chapter. A brief overview of antenna systems for V2V broadcast communications is given in Chapter 4. Furthermore, the feasibility of different multi-antenna schemes in V2V broadcast is discussed. The EDCA scheme is described in detail in Chapter 5 with a discussion on its performance. The sector antenna setup used to improve the PSR in dense vehicular scenarios is also introduced in the chapter. Finally, the author's contributions are summarized in Chapter 6.

Chapter 2

Vehicular Channels

A thorough understanding of vehicular channels is necessary to design and evaluate vehicular communication systems. This chapter discusses the characteristics of vehicular channels and gives an overview of some of the vehicular channel models.

2.1 Wireless Channels

A time-varying wideband wireless channel is represented as a time-varying impulse response $h(t, \tau)$, where t is the absolute time and τ is the delay of the multipath components (MPCs). Fourier transforming $h(t, \tau)$ with respect to τ results in the time-varying transfer function $H(t, f)$.

Wireless channels can be described in terms of three contributing factors, namely, i) path-loss, ii) shadowing, and iii) small-scale fading [36, Ch. 2]. Path-loss is the attenuation of signal power as a function of distance from a transmitter, and is dependent on the carrier frequency and the propagation environments. Shadowing, also known as large-scale fading, is the attenuation of signal power caused by the obstacles between a transmitter and a receiver. Constructive and destructive additions of MPCs cause signal variations over distances in the order of signal wavelengths, which is referred to as small-scale fading. Over the duration of a frame, the path-loss and shadowing are approximately constant and as a consequence, small-scale fading is the main contributor to channel variations over the duration of a frame.

The wide sense stationary uncorrelated scattering (WSSUS) assumption is commonly used to simplify the correlation functions and analysis of wideband channels. Wide sense stationary (WSS) means that the mean and the time correlation function of each tap measured at two different times, t and $t + \Delta t$, depends only on the difference Δt. Uncorrelated scattering (US) means that a multipath component with delay τ_1 is uncorrelated with all multipath components with a different delay $\tau_2 \neq \tau_1$. The US assumption results in the channel transfer function $H(t, f)$ being WSS in f [37, Section 6.4]. As a consequence, the time-frequency correlation function of a wideband channel under the

WSSUS assumption is given by

$$R_H(t, t+\Delta t, f, f+\Delta f) = E\left\{H^*(t,f)H(t+\Delta t, f+\Delta f)\right\} \tag{2.1}$$
$$= R_H(\Delta t, \Delta f) \tag{2.2}$$

where $E\{\cdot\}$ denotes the expectation operation. The autocorrelation functions $R_{H,\mathrm{f}}(\Delta f) \triangleq R_H(0, \Delta f)$ and $R_{H,\mathrm{t}}(\Delta t) \triangleq R_H(\Delta t, 0)$ form a Fourier transform pair with the power delay profile [36, Section 3.3.1-2] and Doppler power spectrum of the channel [36, Section 3.3.3], respectively.

Coherence bandwidth B_{coh} is the contiguous band of frequencies over which the correlation function $|R_{H,\mathrm{f}}(\Delta f)| \geq \eta_{\mathrm{f}}$. Different values of η_{f} have been used in the literature to define B_{coh}. Coherence bandwidth can be approximated in terms of the root mean square (rms) delay spread τ_{rms} and is given by

$$B_{\mathrm{coh}} \approx 1/\tau_{\mathrm{rms}}. \tag{2.3}$$

Coherence time T_{coh} is the duration over which the correlation function $|R_{H,\mathrm{t}}(\Delta t)| \geq \eta_{\mathrm{t}}$. Different values of η_{t} have been used in the literature to define T_{coh}. Coherence time can be approximated in terms of the rms Doppler spread $B_{\mathrm{D,rms}}$ and is given by

$$T_{\mathrm{coh}} \approx 1/B_{\mathrm{D,rms}}. \tag{2.4}$$

The above relations indicate the order of magnitude relation between the quantities. Different scaling factors, maximum Doppler shift $B_{\mathrm{D,max}}$ (also referred to as Doppler spread), and maximum excess delay τ_{max} are used to define coherence time and bandwidths in the literature [36–38]. Nevertheless, the important thing to note is the inverse relationships in (2.3) and (2.4).

2.2 Characteristics of Vehicular Wireless Channels

Vehicular wireless channels in V2V scenarios exhibit different characteristics in comparison to the traditional cellular channels. A major factor contributing to this difference is the heights at which the transmitter and receiver antennas are mounted. In cellular scenarios, the base station antenna is located at a much greater height than a user equipment and there are few immediate scatterers around. Whereas, in a V2V scenario both the transmitter and receiver antennas are located at similar heights, and can be surrounded by both fixed and mobile scatterers resulting in many significant multipath components. Furthermore, the transmitter, the receiver, and other reflectors may be moving with high velocities in opposite directions resulting in large Doppler spreads that give rise to highly time-varying channels. A detailed account on the characteristics discussed above and their effect on communication system design is given in [8].

Geometry and physical environment of the traffic scenario, and the driving directions of the transmitter and the receiver have a huge impact on the characteristics of the vehicular channels. A strong line-of-sight (LOS) component can be present in a highway scenario, which could be completely absent in an urban intersection scenario. Doppler

spreads can vary largely depending on the relative velocities between the transmitter and the receiver, and the other vehicles [8]. Owing to the scenario specific characteristics of vehicular channels, measurements in different traffic scenarios have been conducted in several campaigns [9–15]. In [14], a local scattering function is used to analyze the channel measurements from the DRIVEWAY 2009 campaign, and to compute the rms delay and rms Doppler spreads of the measured channels. The rms delay and rms Doppler spreads are found to vary over a large range of values for different scenarios. Rms Doppler spreads, $B_{\mathrm{D,rms}} > 900\,\mathrm{Hz}$ and rms delay spreads, $\tau_{\mathrm{rms}} > 900\,\mathrm{ns}$ are reported, which indicate the highly time- and frequency-varying nature of vehicular channels. In [15], V2V channels are broadly classified into three groups, i) LOS: in this scenario, there exists a LOS link between a transmitter and a receiver; ii) obstructed LOS (OLOS): in this situation, the LOS link between a transmitter and a receiver is partially or completely blocked by another vehicle; iii) NLOS: in this scenario, the LOS link and many MPCs with significant power are completely blocked by a larger obstacle such as a building. In a traffic scenario, V2V channels can transit between the above mentioned situations. For example, in a traffic intersection the V2V channel can transit from NLOS to LOS and vice-versa.

2.3 Channel Models

In this section, some vehicular channel models are described with focus on small-scale fading. Three modeling approaches are discussed, namely, i) deterministic, ii) stochastic, and iii) geometry-based stochastic. For details on path-loss and shadowing models in vehicular communications see [13, 15, 39, 40].

2.3.1 Deterministic Ray-Tracing

In ray-tracing, a ray approximation of Maxwell's equations is used along with the electromagnetic properties of the objects to compute the signal contributions at a receiver. In the ray approximation, electromagnetic waves are modeled as rays and all the rays (direct ray and rays with multiple reflections) that can transfer energy from a transmitter to a receiver are determined. Subsequently, the attenuation of each ray due to free space propagation and interactions with the objects is computed. The contributions of all the rays are then summed up at the receiver. The ray-tracing approach can accurately simulate wireless channels at the cost of the computational complexity involved in the computation of the contribution of each ray and the requirement of accurate characterization of the electromagnetic properties of the objects in the environment.

The ray-tracing approach to simulate and study the characteristics of vehicular channels has been employed in [31], where a three-dimensional ray-tracing tool called Virtual Drive is developed. The tool allows to create different road traffic scenarios by placing typical objects according to a desired density. The tool has also been used to study the optimal placement of antennas on a vehicle in [31].

2.3.2 Stochastic Channel Models

Stochastic channel models model the long term statistics of the channels in terms of the probability distribution functions (pdfs) and correlation functions of the MPCs. Although stochastic models do not allow the simulation of a specific instance of a wireless channel, they are extensively used for analyzing the statistical performance metrics of communication systems. These small-scale fading models do not include the attenuation due to path-loss and shadowing.

The WSSUS assumption is commonly used in tapped-delay line stochastic channel models [37]. The time-varying impulse response of a tapped-delay line channel is given by

$$h(t,\tau) = \sum_{l=1}^{L} a_l(t)\delta(\tau - \tau_l),$$

where L is the number of taps, $a_l(t)$ and τ_l are the time-varying complex coefficient and delay of the lth tap, respectively; and $\delta(\cdot)$ is the Dirac delta function. A pdf and autocorrelation function are assigned to each time-varying tap $a_l(t)$, and the average power of the taps is chosen according to a power delay profile (PDP).

In [11], tapped-delay line channel models for six different V2V traffic scenarios have been developed based on measurements. The models describe each tap with either a Rayleigh or Rician fading distribution and a Doppler power spectrum. Both WSSUS and non-WSSUS stochastic channel models based on measurements are developed in the form of tapped delay line models in [12]. The nonstationarity of the channel taps is modeled using 'persistence processes,' where certain taps are turned on and off according to a two state Markov process. Tap correlation coefficient matrices are specified to account for the correlation between the taps. Although vehicular channels have been shown to exhibit non-WSSUS characteristics [12, 41], they can be regarded as WSSUS over the duration of a frame allowing the use of WSSUS tapped-delay models for performance evaluation. However, the non-WSSUS characteristic of the channels prevents the collection of long term channel statistics in a receiver to facilitate channel estimation.

A time-varying transfer function of one realization of the Highway NLOS stochastic channel model based on channel measurements is shown in Figure 2.1 [42]. The channel has a bandwidth of 10 MHz and spans over a duration of 1.4 ms. The Highway NLOS channel model has a maximum Doppler shift $B_{\mathrm{D,max}} = 886\,\mathrm{Hz}$ and maximum excess delay $\tau_{\max} = 700\,\mathrm{ns}$, exhibiting high time- and frequency-selectivity as seen in the figure.

2.3.3 Geometry Based Stochastic Channel Models

The ray-tracing approach is computationally complex and the tapped-delay line models are not well suited for simulating a specific channel realization. Geometry-based stochastic channel models (GSCMs) allow simulation of a specific channel realization with reduced complexity. In GSCMs, scatterers are placed randomly according to specified statistical distributions and different scattering properties are assigned to them. Simplified ray-tracing is then used to determine the signal contribution of the scatterers at the receiver. Typically, only single or double scattering is considered, which greatly

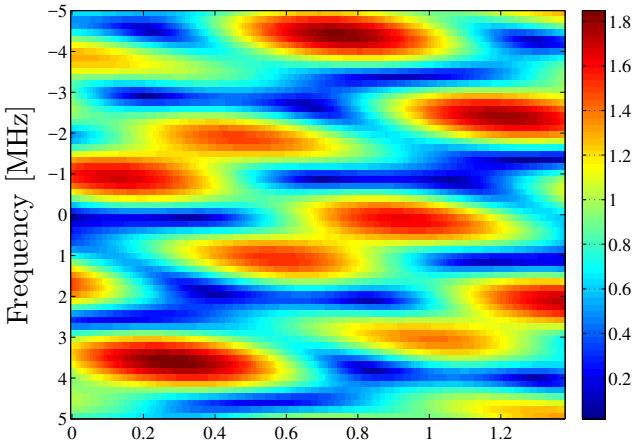

(a) Magnitude

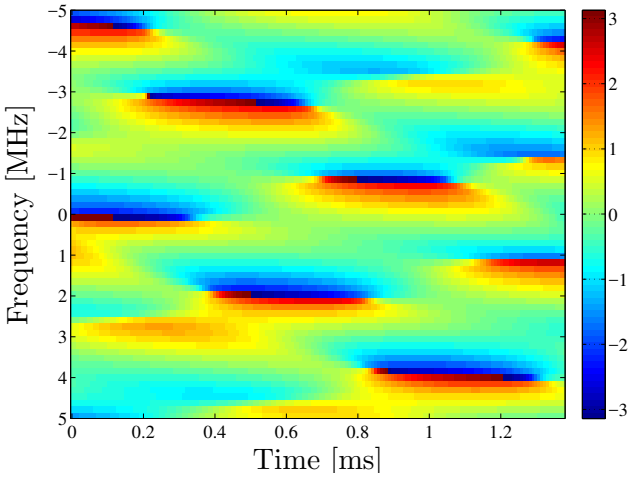

(b) Phase in radians

Figure 2.1: Time-varying transfer function $H(t, f)$ of one instance of the Highway NLOS channel in a time-frequency grid with 10 MHz bandwidth and spanning a duration of 1.4 ms.

reduces the computational complexity [43]. GSCMs offer several benefits: (i) they can handle non-WSSUS channels, (ii) multiple input multiple output (MIMO) properties of the channel can easily be incorporated, and (iii) they provide double directional description of the channel by allowing AOA and angle-of-departure (AOD) description of the MPCs, and the option of including antenna patterns.

A double directional GSCM with a detailed implementation procedure is described in [43]. The double directional, time-variant channel response is modeled as [44]

$$h(t,\tau) = \sum_{i=1}^{N} a_i(t) e^{j\frac{2\pi}{\lambda} d_i(t)} \delta(\tau - \tau_i) \delta(\Omega_R - \Omega_{R,i}) \delta(\Omega_T - \Omega_{T,i}) g_R(\Omega_R) g_T(\Omega_T), \quad (2.5)$$

where $\tau_i, \Omega_{R,i}$, and $\Omega_{T,i}$ are the excess delay, AOA and AOD of the ith path; $g_T(\Omega_T)$ and $g_R(\Omega_R)$ are the transmitter and receiver antenna directive gain patterns, respectively; $a_i(t)$ and $d_i(t)$ are the complex amplitude and the distance of the ith path, λ is the wavelength, and $e^{j\frac{2\pi}{\lambda} d_i(t)}$ is the distance-induced phase shift. In [43], the impulse response is categorized into four parts based on different types of scatterers: (i) the LOS component which might also include other static components, (ii) discrete components resulting from mobile objects (MD), (iii) discrete components resulting from static objects (SD), and (iv) diffuse components (DI). The impulse response in (2.5) is then split in four parts as

$$h(t,\tau) = h_{\mathrm{LOS}}(t,\tau) + \sum_{p=1}^{P} h_{\mathrm{MD},p}(t,\tau) + \sum_{q=1}^{Q} h_{\mathrm{SD},q}(t,\tau) + \sum_{r=1}^{R} h_{\mathrm{DI},r}(t,\tau), \quad (2.6)$$

where P, Q, and R are the number of discrete mobile objects, discrete static objects, and diffuse components, respectively. The complex amplitudes in the four different parts are modeled using distance dependent gains and fading distributions which can be determined from channel measurements [43].

2.4 Summary

Relevant channel models have to be chosen to evaluate the performance of vehicular communication systems. Although ray-tracing and GSCM models can model the vehicular channels more accurately than the stochastic channel models, stochastic channel models with WSSUS assumption are still relevant for evaluating the performance of vehicular communication systems as they can be easily simulated and interfaced with transceiver implementations. Also, commercial channel emulators support emulation of stochastic channels which enable us to conduct frame error rate (FER) performance tests on hardware transceiver implementations operating in real time. Considering these advantages, stochastic channel models are used in the thesis and the attached papers to evaluate the performance of different channel estimation algorithms.

Chapter 3

Channel Estimation in IEEE 802.11p

Channel estimation in a communication system depends on the modulation parameters, pilot pattern, the channels over which they are deployed, and the channel estimation algorithms. In this chapter, the IEEE 802.11p standard and its pilot pattern are discussed. Subsequently, an overview of the channel estimation schemes that have been studied for 802.11p is given. A modified frame format with complementary pilots, which is obtained by the backward standard-compatible cross-layered pilot insertion scheme, proposed in Paper A and Paper B is introduced.

The backward compatibility of the pilot insertion scheme and its implementation feasibility is verified by implementing a receiver that can utilize the complementary pilots on a hardware platform. Some important aspects of the hardware implementation are also discussed in the chapter.

3.1 IEEE 802.11p

The PHY layer of 802.11p uses orthogonal frequency-division multiplexing (OFDM) with $N = 64$ subcarriers. Channel spacing of 10 MHz is specified for safety related applications [45]. The parameters of 802.11p for 10 MHz channel spacing are shown in Table 3.1. The orthogonality duration (T) is the duration over which the subcarriers are orthogonal and the subcarrier spacing (Δ_f) is the separation of the subcarriers in frequency. The total duration of an OFDM symbol (T_{SYM}) is the sum of the orthogonality duration (T) and the duration of the cyclic prefix (T_{CP}).

Two guidelines are normally followed in the design of an OFDM system. Firstly, the duration of the cyclic prefix T_{CP} has to be greater than the maximum excess delay of the wireless channel $\tau_{\max}$ to completely eliminate intersymbol interference between consecutive OFDM symbols [46, Section 1.4], i.e.,

$$\tau_{\max} < T_{\mathrm{CP}} = 1.6\,\mu\mathrm{s}.$$

Secondly, the subcarrier spacing Δ_f has to be much larger than the maximum Doppler

Table 3.1: Parameters of IEEE 802.11p in 10 MHz channel spacing

Parameter	Symbol	Value
Number of subcarriers	N	64
Subcarrier spacing	Δ_f	156.25 kHz
Orthogonality duration	T	6.4 μs
Duration of cyclic prefix	T_{CP}	1.6 μs
Total symbol duration	T_{SYM}	8 μs

shift $B_{\mathrm{D,max}}$ to keep the intercarrier interference negligible [46, Section 2.2], i.e.,

$$B_{\mathrm{D,max}} \ll \Delta_f = 156.25\,\mathrm{kHz}.$$

The maximum excess delay values and the Doppler shifts reported in the channel measurement campaigns [11, 12, 14] satisfy the above two guidelines for the 10 MHz channel spacing.

The encoding process of an 802.11p OFDM symbol is described in [17] and Paper A. The 802.11p standard supports eight different modulation and coding schemes (MCSs) for encoding the data bits. The MCS with code rate 1/2 and QPSK modulation is specified for safety applications and will be the focus of the thesis. Pilot symbols that are known to receivers are multiplexed with the data symbols to aid in channel estimation. Figure 3.1 shows a standard 802.11p frame (SF) in a subcarrier-time grid. Two identical OFDM symbols referred to as long training (LT) are at the beginning of the frame. The SIGNAL symbol carries the information regarding the length of the packet, and the MCS used for encoding the data bits. The DATA OFDM symbols follow the SIGNAL symbol and each of them carry four pilots referred to as comb pilots. The frame also consists of 10 short identical sequences that precede the LT symbols (not shown in figure), these are used by the receiver for frame detection, synchronization, and automatic gain control.

At the receiver, the cyclic prefix (CP) of the received time domain OFDM symbol is discarded and an N-point DFT is performed to obtain the frequency domain symbols. Assuming perfect frequency and time synchronization, and that the duration of the CP is longer than the channel impulse response, the received frequency domain symbols after the DFT operation are given by [47, Section 8.3]

$$y[m,k] = h[m,k]x[m,k] + w[m,k], \tag{3.1}$$

where $h[m,k]$ is the channel frequency response at the kth subcarrier of the mth OFDM symbol and $w[m,k]$ is the frequency domain independent and identically distributed complex additive white Gaussian noise sample with zero mean and variance N_0. The effect of intercarrier interference is neglected since the channel can be considered to be approximately time-invariant over the duration of one OFDM symbol. The relation can be further written in vector notation as

$$\mathbf{y}_m = \mathbf{X}_m\mathbf{h}_m + \mathbf{w}_m, \tag{3.2}$$

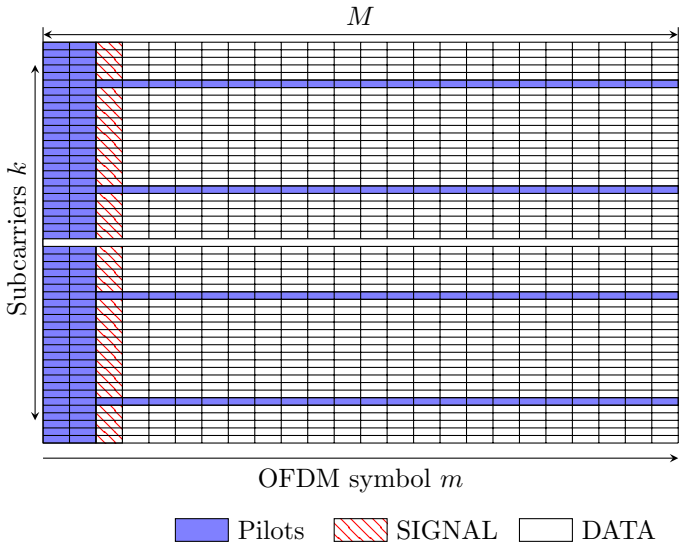

Figure 3.1: A standard 802.11p frame in subcarrier-time grid showing the position of the pilots and the data symbols.

where $\mathbf{X}_m$ is a diagonal matrix of transmitted quadrature amplitude modulation (QAM) symbols in the mth OFDM symbol; $\mathbf{h}_m$ and $\mathbf{w}_m$ are the column vectors of the channel frequency responses and noise samples in the mth OFDM symbol, respectively.

An estimate of the channel frequency response $h[m, k]$ is necessary to perform coherent detection. Practical wireless communication systems utilize pilot symbols to perform channel estimation. Pilots that are suitably placed in the subcarrier-time grid enable channel estimation with low mean squared error (MSE) using low complexity algorithms [48]. As seen in Figure 3.1, the pilots sample the channel frequency response $h[m, k]$ at all subcarriers only at the beginning of the frame and at four comb pilot subcarriers for the rest of the frame. This pilot pattern is well suited for static indoor environments for which the 802.11a was originally designed. When the channel is static, it is only necessary to estimate the channel at all the subcarriers in the beginning of a frame and use it for decoding the data in the rest of the frame. The comb pilots can be additionally used to correct slow phase or frequency drifts. Availability of channel estimates at the beginning of a frame eliminates the need for buffering of data symbols and simplifies receiver implementation. Owing to these aspects, the pilot pattern in 802.11p is an efficient design for static indoor environment.

As discussed in Chapter 2, vehicular channels are not static and if channel estimation is to be performed by using pilots alone, the pilots should be placed according to the coherence time and coherence bandwidth of the wireless channel. The maximum pilot

separation in frequency domain (in number of subcarriers) should satisfy

$$\Delta_{\mathrm{p},f} \leq \frac{B_{\mathrm{coh}}}{\Delta_f} \approx \frac{1/\tau_{\mathrm{rms}}}{\Delta_f}, \tag{3.3}$$

and the separation of pilots in time domain (in number of OFDM symbols) should satisfy

$$\Delta_{\mathrm{p},t} \leq \frac{T_{\mathrm{coh}}}{T_{\mathrm{SYM}}} \approx \frac{1/B_{\mathrm{D,rms}}}{T_{\mathrm{SYM}}}. \tag{3.4}$$

The requirements in (3.3) and (3.4) give an insight into a suitable choice of pilot spacing based on coherence time and coherence bandwidth. They are not, however, absolute requirements.

Rms Doppler spreads, $B_{\mathrm{D,rms}} > 900\,\mathrm{Hz}$ and rms delay spreads, $\tau_{\mathrm{rms}} > 900\,\mathrm{ns}$ have been reported from the channel measurements [14, Table II]. For these values, the above mentioned conditions are not satisfied for the 802.11p pilot pattern, where $\Delta_{\mathrm{p},f} = 14 > (B_{\mathrm{coh}}/\Delta_f) \approx 7$, and no pilots are present on the data subcarriers after the LT symbols. As a consequence, estimation of vehicular channels in 802.11p becomes a challenging task.

Several solutions have been proposed to address the problem of channel estimation in 802.11p systems in highly time- and frequency-varying channels. A set of solutions propose different pilot patterns that provide more support for channel estimation and thereby require changes in the 802.11p PHY layer specification [18–20]. The other set of solutions employ decision feedback and turbo equalization techniques to improve the FER performance of the receiver while utilizing the existing pilot pattern [21–28].

3.2 Channel Estimation Schemes

Channel estimation in OFDM communication systems is a well researched topic [46, 48–54]. However, channel estimation in 802.11p OFDM systems is constrained by the pilot pattern that is ill-suited for highly time- and frequency-varying channels. In this section, some important channel estimation schemes relevant for the 802.11p systems are presented.

Channel estimation schemes are broadly classified into blind, pilot aided, and decision feedback. Pilot aided estimation schemes rely on the data known at the receiver for channel estimation. Decision feedback methods rely on the pilots for initial channel estimation and on the bit or constellation symbol decisions afterwards for updating the initial channel estimates. Blind channel estimation schemes do not rely on the pilots and are seldom used in practical systems due to their higher complexity and poor performance, and hence not studied in this section [37, Section 16.7].

3.2.1 Pilot Aided Estimation

In block least-squares (LS) scheme, LS channel estimates are calculated using the two identical LT symbols and are averaged to obtain less noisy channel estimates given by

$$\hat{\mathbf{h}}_{\mathrm{LT-LS}} = \mathbf{X}_{\mathrm{LT}}^{-1}\left(\frac{\mathbf{y}_1 + \mathbf{y}_2}{2}\right), \tag{3.5}$$

where $\mathbf{y}_1$ and $\mathbf{y}_2$ are the two received LT symbols, and $\mathbf{X}_{\mathrm{LT}}$ is a diagonal matrix of BPSK pilot symbols in one LT OFDM symbol. It is assumed that the channel frequency responses $\mathbf{h}_1$ and $\mathbf{h}_2$ are identical.

The block linear minimum mean squared error (LMMSE) channel estimates which are obtained by smoothing the LS estimates are given by [49, 52]

$$\hat{\mathbf{h}}_{\mathrm{LT-LMMSE}} = \mathbf{R}_{hh}\left(\mathbf{R}_{hh} + \frac{N_0}{2}\left(\mathbf{X}_{\mathrm{LT}}\mathbf{X}_{\mathrm{LT}}^{\mathsf{H}}\right)^{-1}\right)^{-1}\hat{\mathbf{h}}_{\mathrm{LT-LS}}, \tag{3.6}$$

where $\mathbf{R}_{hh} = E\{\mathbf{h}\mathbf{h}^{\mathsf{H}}\}$ is the channel autocorrelation. If $\mathbf{R}_{hh}$, $\mathbf{X}_{\mathrm{LT}}$, and N_0 are known beforehand, the estimator matrix can be precomputed and stored. The block LS and LMMSE channel estimates can be used for detecting the data over the rest of the frame. These methods are suitable when the variation of the channel over the frame duration is insignificant.

In [50, Section 4.3], LMMSE interpolation is described for channel estimation where the channel estimate at a data symbol position is obtained as a linear combination of LS channel estimates at the pilot positions. The LS channel estimates at pilot positions are arranged in a vector $\hat{\mathbf{h}}_{\mathrm{p}}$ and the channel coefficients to be estimated in the vector form $\hat{\mathbf{h}}_{\mathrm{d}}$ are given by

$$\hat{\mathbf{h}}_{\mathrm{d}} = \mathbf{R}_{\mathrm{dp}}\mathbf{R}_{\mathrm{pp}}^{-1}\hat{\mathbf{h}}_{\mathrm{p}}, \tag{3.7}$$

where $\mathbf{R}_{\mathrm{dp}} = E\{\mathbf{h}_{\mathrm{d}}\mathbf{h}_{\mathrm{p}}^{\mathsf{H}}\}$ and $\mathbf{R}_{\mathrm{pp}} = E\{\hat{\mathbf{h}}_{\mathrm{p}}\hat{\mathbf{h}}_{\mathrm{p}}^{\mathsf{H}}\}$. In the same work, low rank approximations based on single value decomposition are discussed to reduce the complexity of the estimators in (3.6) and (3.7).

3.2.2 Decision Feedback

Decision feedback based methods for 802.11p employ pilot aided channel estimation schemes to obtain channel estimates at the beginning of the frame and use these estimates to make decisions on bits or symbols. Consequently, the decisions are used to update the initial channel estimates. Figure 3.2 shows the schematic structures of generic decision feedback estimators where the symbol decisions, and bit decisions or a-posteriori probabilities (APPs) of the coded bits are used for updating the channel estimates.

In [21], an early work on supporting mobility in 802.11a, a decision directed channel estimation scheme is proposed. The data bits detected at the output of the channel decoder using the initial channel estimates are reencoded, reinterleaved, and remapped to regenerate the transmitted constellation symbols. The regenerated complex symbols

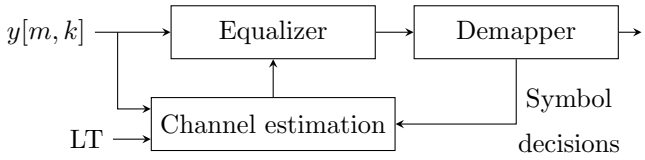

(a) Constellation aided

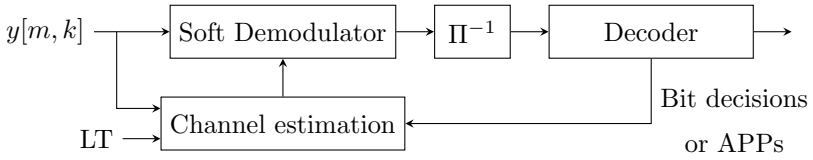

(b) Bit decision aided

Figure 3.2: Schematic structures of decision feedback channel estimators.

are treated as pilot symbols and the corresponding received symbols are used to obtain new channel estimates. The new channel estimates and the previous channel estimates are combined using different weights to compute updated channel estimates. The optimal weights were determined empirically for a specific channel model, update rate, and signal-to-noise power ratio (SNR).

A decision directed channel estimation scheme referred to as spatial temporal averaging (STA) is described in [23]. In STA, initial channel estimates obtained from the LT symbols are used to detect the transmitted constellation symbols of the following received OFDM symbol. The detected symbols are then used to obtain new channel estimates. The new channel estimates are averaged in frequency and in time with weights determined from channel characteristics to form updated channel estimates. In comparison with the method in [21], STA does not use the decoded bits to regenerate the transmitted constellation symbols and is hence computationally less complex. A channel estimation scheme named constructed data pilot (CDP) that is based on the assumption that the channel coefficient of a received symbol is highly correlated with that of the previous symbol is proposed in [24]. In CDP, the validity of the newly computed channel estimate using symbol decisions is verified and if it is found to be invalid, previously computed channel estimate is retained for the channel update. This step tries to prevent a wrong update of the estimate in case the symbol detected is incorrect. The STA and CDP methods show improvements in the FER performance in comparison to the block LS method. However, in [23] and [24], the FER performance of the STA and CDP schemes has not been compared against the case with perfect channel state information (CSI).

Turbo equalization makes use of the turbo principle to jointly detect the data and estimate the channel [55]. A receiver structure, similar to the structure shown in Figure 3.2(b), that uses turbo equalization is discussed in [27]. In turbo equalization,

initial likelihood ratios of coded bits are computed using the initial channel estimates and fed into a soft-input soft-output channel decoder. The soft-output bits are then used along with the initial channel estimates to update the channel estimates. The process of decoding and updating the channel estimates is iterated until a certain stopping criterion is met. An iterative channel estimation scheme that uses generalized discrete prolate spheroidal sequences is shown to provide FER performance very close to the case with perfect CSI in [26]. It has also been shown in the same work that the number of iterations required can be reduced by introducing a postamble at the end of the frame. A factor graph based iterative receiver with reduced complexity is described in [28]. Although good FER performance is reported for varying frame lengths, the FER is still far away from the case with perfect CSI (more than 4 dB difference in SNR). Also, it is seen from the results that the number of iterations required to achieve a fixed bit error rate (BER) increases when the frame length increases. Similar to the results in [26], the number of iterations required to achieve a fixed BER in [28] is shown to reduce with the inclusion of a postamble. Both studies indicate the usefulness of more pilots to reduce latency in iterative receiver structures. Also, pilots distributed throughout the frame allow iterative equalization and detection over a smaller portion of the frame.

3.3 Cross-layered Pilot Insertion Scheme

Channel estimation schemes, such as block LS and block LMMSE, based only on the standard 802.11p pilots perform poorly in highly time- and frequency-varying channels, and the FER performance improves very slowly with SNR as shown in Papers A and B. The FER performance of the low complexity decision feedback methods such as STA and CDP is far from the case with perfect CSI as shown in Paper B. In the case of turbo or iterative equalization, where performance close to the case with perfect CSI is obtained, the algorithms are complex. Pilots distributed throughout the frames are beneficial to perform robust channel estimation using low complexity algorithms [48]. Frame formats where the pilots are distributed throughout the frame have been proposed for vehicular communications. Three pilot patterns referred to as enhanced pilot patterns and periodically inserted pilot OFDM symbols referred to as midambles are proposed in [18]. The concept of midambles is revisited in [19], where a channel tracking algorithm using the midambles is discussed.

A cross-layered pilot insertion scheme to introduce complementary pilot OFDM symbols, referred to as pseudo training (PT) symbols, into the SF is proposed in Papers A and B. In contrast to the pilot schemes introduced in [18–20], the proposed scheme is backward compatible with standard 802.11p transceivers. A modified receiver can make use of the inserted complementary training symbols for robust channel estimation. A standard receiver treats the complementary training symbols as data and passes the entire frame to the higher layers. A standard 802.11p transceiver needs a software/firmware update in the logical link control (LLC) layer that is immediately above PHY and MAC layers (that are typically implemented in hardware and cannot be modified) to insert/remove the PT symbols. Since the proposed pilot insertion scheme is backward compatible, it provides more support for channel estimation while allowing older transceivers to co-exist.

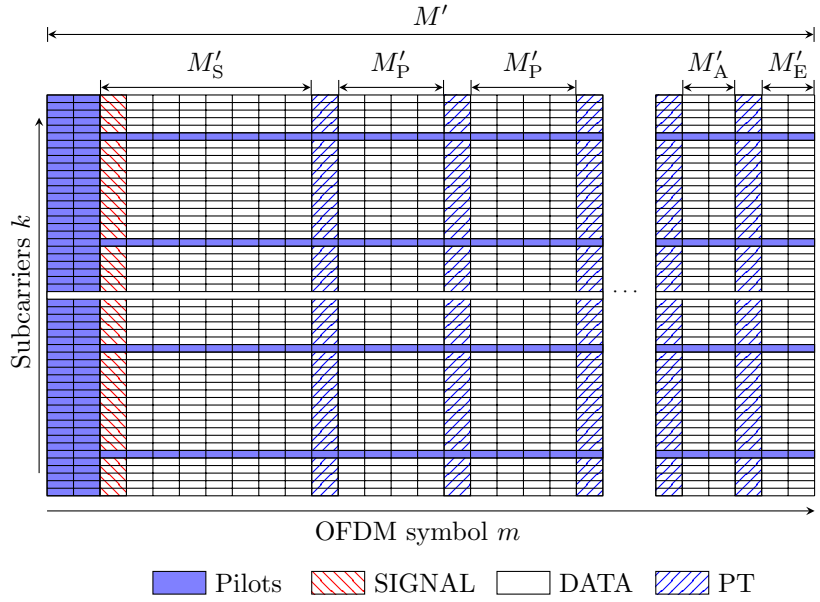

Figure 3.3: A modified 802.11p frame in subcarrier-time grid showing the position of the pilots, the data symbols and the inserted PT symbols.

The proposed modified 802.11p frame (MF) is shown in a subcarrier-time grid in Figure 3.3. The procedure to insert the PT symbols has been described in Papers A and B. The number of OFDM symbols between two periodically inserted PT symbols is denoted by M'_{P}, which is the design parameter of the MF and can be made adaptive depending on the channel conditions or the reliability requirement of an application. The number of OFDM symbols between the LT symbols and the first PT symbol is denoted by M'_{S}, which in some cases can be larger than M'_{P} due to the insertion of the SIGNAL symbol, SERVICE field, and MAC header by the layers below the LLC sublayer. Also, depending on the length of data packet, the frame in the end may consist of less than M'_{P} OFDM data symbols after the periodically inserted PT symbols. In that case, one additional PT symbol is inserted after the periodically inserted training at the end of the frame. The number of OFDM symbols between the final periodically inserted PT symbol and the additional PT symbol is denoted by M'_{A}. Since the cyclic redundancy check (CRC) and the termination bits are appended to the end of the frame by the layers below the LLC layer, the frame consists of M'_{E} OFDM symbols after the final PT symbol as shown in the figure.

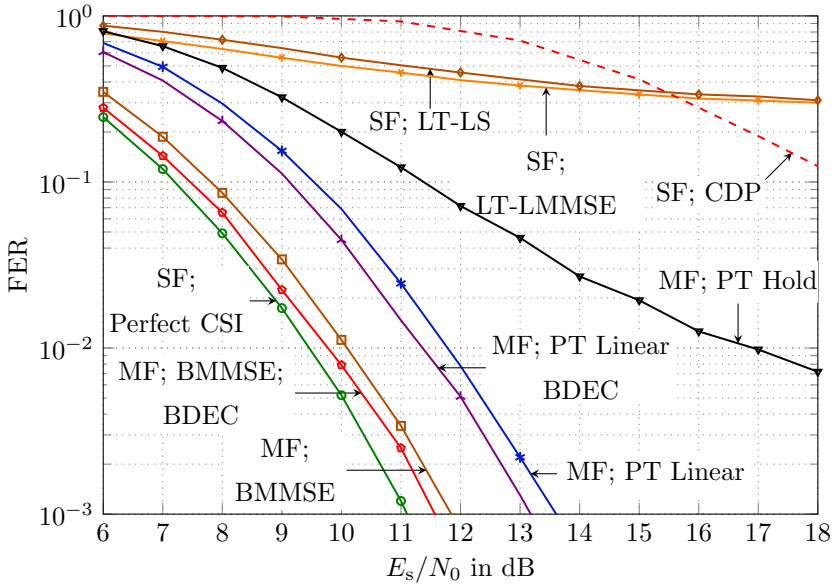

Figure 3.4: Simulation FER results of SFs ($M = 35$) and MFs ($M = 37$) for different channel estimation schemes in the EXP channel with $v = 100$ km/h.

3.4 Comparison of Channel Estimation Schemes

The FER performance of some of the channel estimation schemes is compared in this section. The receiver and the EXP channel model described in Paper B are used. The EXP channel model is a stochastic channel model having an exponentially decaying PDP with $\tau_{\text{rms}} = 0.4\,\mu$s. The tap gains are independent zero mean complex Gaussian with autocorrelation function $\alpha_l \text{J}_0(2\pi(v/\lambda)t)$, where α_l is the average power of the lth tap, v is the relative velocity between the transmitter (TX) and the receiver (RX), λ is the wavelength of the electromagnetic carrier wave of frequency $f_c = 5.9\,$GHz. Hence, each tap exhibits Rayleigh fading with the classical Clarke's power spectrum. The MCS with QPSK mapping and code rate 1/2 is adopted for the safety applications and is the focus of the FER results. The FER results in this section are plotted against E_s/N_0, where E_s is the average energy of the frequency domain symbols $x[m, k]$.

Figure 3.4 shows the FER performance of different channel estimation schemes in the EXP channel with $v = 100\,$km/h. An SF with $M = 35$ OFDM symbols is transmitted. $M'_{\text{S}} = M'_{\text{P}} = 16$ is chosen for the MFs, which corresponds to $M' = 37$ in Figure 3.3 for the same length of data. The MF contains no additional PT symbol after the final periodic PT symbol and $M'_{\text{E}} = 1$. The FER of the SF in case of LT-LS and LT-LMMSE channel estimation schemes decreases very slowly with increasing SNR. Since the PT symbols are inserted periodically in an MF, two consecutive PT symbols and the data OFDM symbols sandwiched between them can be considered as a block and channel

estimation can be performed for each of the blocks separately. The block MMSE estimation (BMMSE) scheme for the MFs, described in Paper A, that performs blockwise LMMSE interpolation has an FER performance that is close to the case with perfect CSI. However, this scheme requires the knowledge of channel correlation functions and involves large matrix operations. FERs of PT Hold and PT Linear channel estimation schemes for MFs, described in Paper B, are also shown Figure 3.4. In the PT Hold scheme, the LS channel estimates at a PT symbol are used for decoding the data until the next PT symbol is received. In the PT Linear scheme, the channel estimates between two consecutive PT symbols are computed using linear interpolation of the LS estimates at the PT symbols. PT Hold and PT Linear schemes are computationally simple and do not require the knowledge of the channel correlation functions. As seen in the figure, PT Linear scheme provides significant FER performance gain over the LT-LS and LT-LMMSE channel estimation schemes. The FER performance in MFs can be further improved by performing blockwise Viterbi decoding as described in Paper A. The figure shows the performance improvement of the BMMSE and PT Linear schemes with block decoding (BDEC). FER performance of the CDP channel estimation scheme proposed in [24] is also shown in the figure. The FER performance of the CDP scheme improves at higher SNRs. An FER close to 10^{-2} is achieved at $E_\mathrm{s}/N_0 = 25\,\mathrm{dB}$ (not shown in the figure), which is significantly worse than the perfect CSI case operating at around 9.5 dB.

The number of OFDM symbols between two consecutive PT symbols, M'_P, is a design parameter of the MFs. Frequent insertion of PT symbols increases the overhead due to pilots. Whereas, a larger M'_P increases the buffer size required to store the data symbols between the consecutive PT symbols. Also, the FER performance provided by an M'_P is dependent on the channel estimation scheme used at the receiver. For a low complexity channel estimation scheme that does not use the channel correlation functions, or iterative decoding and equalization strategies, PT symbols may have to be placed more frequently than specified by the requirement stated in (3.4). Figure 3.5 shows the FER performance of the PT Linear channel estimation scheme for different values of M'_P in EXP channel with $v = 200\,\mathrm{km/h}$. An SF with $M = 178$ is transmitted and the lengths of the corresponding MFs are $M' = \{227, 204, 190, 185, 182, 181\}$ for $M'_\mathrm{P} = \{4, 8, 16, 30, 45, 60\}$, respectively. The FER of the SF with LT-LS scheme is approximately equal to 1 for all SNRs. The FER performance of the PT Linear scheme for $M'_\mathrm{P} = \{4, 8, 16\}$ follows the performance of the SF with perfect CSI with an offset in SNR. The FER performance of the PT Linear scheme starts to degrade with $M'_\mathrm{P} \geq 30$ and the FER is close to 1 for $M'_\mathrm{P} = 60$.

As seen in Figure 3.5, the FER performance does not improve substantially when M'_P is reduced from 16 to 4. This is due to the fact that, when the consecutive PT symbols are placed such that the channel variation between them is approximately linear, the mean squared channel estimation error in the PT Linear scheme is dominated by the estimation error of the LS estimates at the PT symbol positions and the error due to linear approximation is negligible. As a consequence, the mean squared channel estimation error in the PT Linear scheme is approximately constant when M'_P is reduced from 16 to 4, and the FER performance does not improve substantially. The PT Linear channel estimation was chosen in Paper B since it is readily implemented in hardware. Other

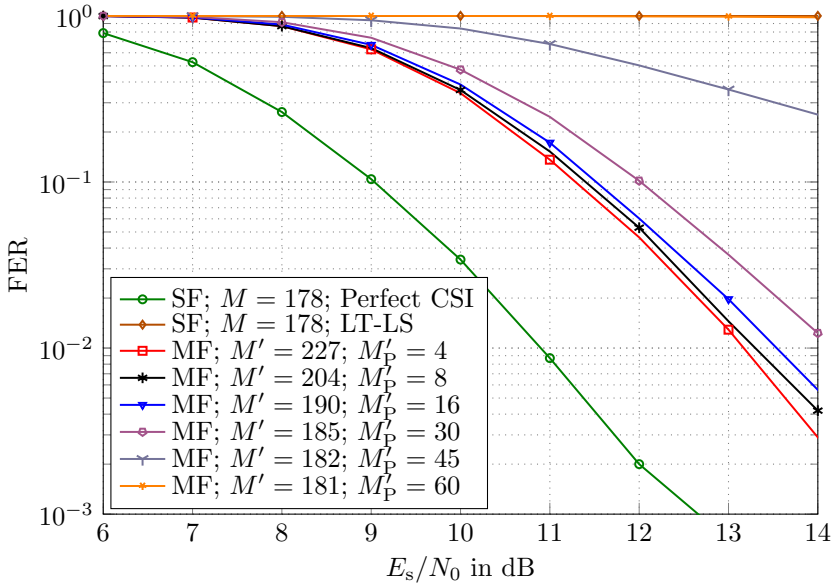

Figure 3.5: Simulation FER results of MFs using PT Linear interpolation scheme for different M'_P in the EXP channel with $v = 200$ km/h.

channel estimation schemes with reasonable complexity can be implemented to further improve the FER performance.

Figure 3.6 shows the FER performance as a function of relative vehicular velocity v in EXP channel at a fixed SNR, $E_s/N_0 = 12$ dB. An SF with $M = 178$ is transmitted, and $M'_P = 16$ is chosen for the MF, which corresponds to $M' = 190$. In the case of perfect CSI, the FER performance is approximately constant with increasing v. The FER of the LT-LS scheme rapidly increases to 1 with increasing v. This is due to the fact that the channel is estimated only at the beginning of the frame. The FER performance of the PT Linear scheme slowly degrades with increasing v.

3.5 Hardware Implementation

A modified receiver capable of utilizing the PT symbols in MFs is implemented in HIRATE, a field programmable gate array (FPGA) based hardware platform developed at Fraunhofer Heinrich Hertz Institute, Berlin [56]. The architecture of the hardware platform is briefly described in Paper B. The modified receiver was implemented by extending an existing HIRATE implementation of a standard compliant 802.11p transceiver. FER measurements have been performed by interfacing the implemented transceiver with a channel emulator. Also, the backward compatibility of the pilot insertion scheme was verified by testing the implemented transceiver with a commercial 802.11p transceiver.

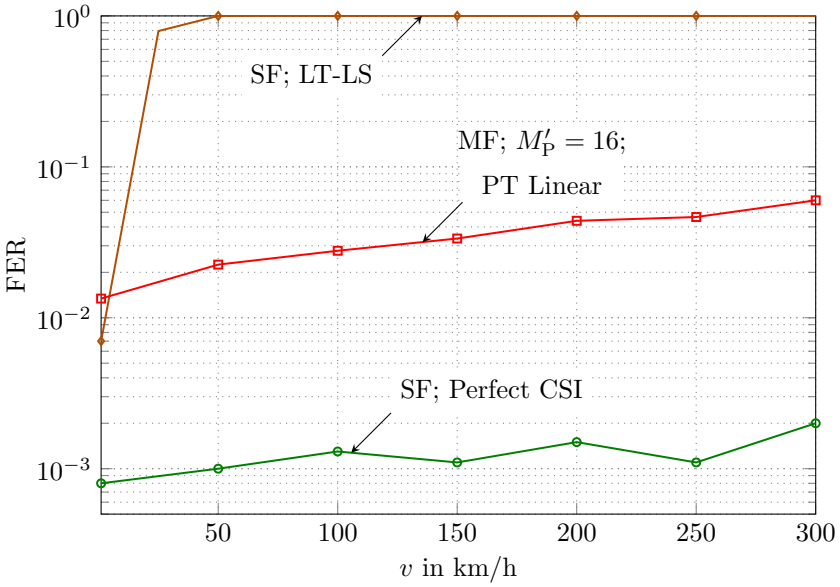

Figure 3.6: Simulation FER results of SFs with $M = 178$ and MFs with $\{M' = 190$ and $M'_{\mathrm{P}} = 16\}$ for different relative velocities in EXP channel. The SNR is fixed to $E_{\mathrm{s}}/N_0 = 12\,\mathrm{dB}$.

The FER results and the verification of backward compatibility have been discussed in Paper B.

In this section, aspects of the hardware implementation work that have not been included in Paper B are discussed. This section points out some generic differences between high level language (HLL) computer simulations and FPGA implementations to communication engineers with no prior experience in FPGA implementation. The content of the section is based on the author's limited experience, an experienced FPGA developer might find it trivial.

3.5.1 Graphical Development

The HIRATE platform is based on a Gidel Procstar III evaluation board with four Altera Stratix FPGAs. The implementation of the transceiver was done in Simulink and MATLAB using a graphical design approach. Altera DSP builder provides a library of standard and advanced blocks in the Simulink environment that can be used to implement the transceiver digital signal processing (DSP) algorithms. The library includes fast Fourier transform (FFT), inverse-FFT, and soft-input Viterbi decoder blocks, which enable rapid prototyping of an 802.11p transceiver. Signals generated during the run time of the Simulink model can be exported to MATLAB-workspace allowing a user to analyze the signals using MATLAB. After the completion and verification of the Simulink

model, it is then converted to hardware description language (HDL) targeted for a wide range of Altera FPGA models with the Altera signal compiler. Similar libraries and development methodologies are supported by other FPGA vendors.

3.5.2 Transition from High Level Language Simulations to FPGA Implementation

Although graphical development requires little or no knowledge of HDLs, FPGA implementation differs from the HLL computer simulations significantly in some aspects. A brief description of the major differences is given below.

1. Parallel/pipeline processing: The system to be implemented in an FPGA platform has to be designed for parallel/pipeline processing. As a first step in transition from HLL simulations to FPGA implementation, the system has to be rearranged to function in parallel/pipeline processing.

2. Indexing: HLLs used for the simulations offer a large flexibility in indexing arrays and matrices. However, in an FPGA implementation, indexing involves usage of counters to generate indices or prestorage of indices in the read only memory (ROM) space.

3. Precision: All the signals in an FPGA implementation have finite and varying bit widths. Using the same precision as in the FPGA implementation for all the variables in the HLL simulations would be helpful in including the effects of limited precision on algorithms.

4. Processing delay: A signal processing operation in an FPGA requires a fixed number of clock cycles and hence the output of the operation is delayed. Owing to the pipelined nature of the implementation, delay introduced by a processing block has to be taken into consideration. Any other signals that are to be processed together with the output of the operation have to be aligned in time according to the delay.

5. Memory: Any signal that cannot be immediately fed to a block for further processing has to be delayed or stored for accessing later. Storing and reading involves generating indices and signals for writing/reading from random access memories (RAMs).

6. Registers: Registers are used to add flexibility into an FPGA implementation. The content of the registers can be changed during the run time of the implementation. Registers allow us to change the operation mode of the implementation or make the constants used in algorithms adaptive. However, the implementation should already include all the elements necessary to adapt according to the values in the registers.

7. Completeness: In baseband HLL simulations of digital communications, frame detection, synchronization, and automatic gain control (AGC) are most often assumed to be perfect. This is a good abstraction for developing algorithms. Nonetheless, if

the end goal is the development and verification of a complete FPGA transceiver implementation, it is necessary to include all the receiver front end operations in the simulations to capture the influence of these operations on the performance of the system.

8. Compilation and emulation: Unlike the compilation of HLLs, the compilation of an FPGA implementation is a tedious task. Care must be taken during the implementation and the design must be thoroughly verified using emulations before the compilation. However, emulation of an entire model, for example an 802.11p receiver, can be very slow since every element in the implementation is emulated for each clock cycle. This makes the verification of the model using statistical metrics such as BER and FER a tedious task.

3.5.3 Analog Components

A brief account of some of the analog components used in the transceiver implementation is given below.

1. Analog-to-digital converters (ADCs) and digital-to-analog converters (DACs): The ADCs and DACs that interface the FPGA inputs/outputs with the analog components have limited bit widths and hence, limited precision and dynamic range. HIRATE uses DACs and ADCs of 16 and 8 bit, respectively.

2. Upsampling and downsampling: The baseband algorithms operate at a sampling rate of 10 MS/s. At the transmitter, the baseband samples at 10 MS/s are upsampled to 160 MS/s, filtered using an FIR filter and then fed to the DAC. At the receiver, the output of the ADC sampled at 160 MS/s is filtered using an FIR filter and downsampled to 10 MS/s.

3. AGC: In the receiver, the ADC has a limited bit width and as a consequence, a limited dynamic range. A disadvantage of OFDM communication systems is the high peak to average power ratio (PAPR). The gain of the AGC has to be adjusted such that the clipping of the peaks and loss of smaller values is minimized. The AGC is configured to control the gain of the amplifier such that the average signal power is at a certain dB level with reference to the full scale of the ADC, denoted by dBFS.

4. Other analog components such as reference clocks, oscillators, up- and down-mixers, and amplifiers also have a huge influence on the performance of the final transceiver implementation. The author has not worked with these components and hence refrains from describing them. Poor electromagnetic shielding of cables and wear-and-tear of connectors can also have undesired effects on the performance and the repeatability of the experiments.

3.5.4 Challenges and Correction Measures

Some of the challenges encountered during the implementation and measurement, and the steps taken to overcome them are briefly discussed below.

1. Debugging: When a change is made to an FPGA implementation, the HDL code has to be regenerated and reintegrated into the entire design for testing on the FPGA platform. If the implementation is large, for example a complete 802.11p receiver, the HDL code generation and integration takes a long time. Therefore, it is necessary to take suitable measures during implementation of a feature so that it can be verified during the execution on FPGA. In HLL simulations, all the intermediate signals can be easily stored and analyzed for errors. However, in an FPGA implementation, if a signal needs to be debugged it has to be stored in the RAM while it is valid during the run time and read later on for debugging. As a consequence, during the implementation of a feature, it is also necessary to implement storing and reading of signals relevant for debugging.

2. Switches: In an FPGA implementation, various blocks of the system are interlinked and designed to work in a parallel/pipeline mode. A newly added feature might render the implementation nonfunctional. To be able to firmly conclude that the problem is due to the newly added feature, it is desirable to have an option for disabling the feature after the final compilation has been done. This can be done by including switches and multiplexers to enable/disable the feature.

3. Measurements: When measurements are performed with the analog components it is important to isolate the interference among the components. Undesired interference among analog components can result in unexpected results and make the verification of the signal processing algorithms a challenging task.

3.5.5 Updates to the Existing Implementation

A receiver capable of utilizing the inserted training symbols was implemented by modifying an existing HIRATE 802.11p implementation. The most important additions and/or modifications performed are listed below.

1. Soft demodulator: The existing implementation used hard decision for demapping the received QPSK symbols to bits. The hard decision is replaced to compute max-log approximations of log-likelihood ratios (LLRs) of the coded bits.

2. Viterbi decoder: Since hard decision was used for demapping, a binary-input Viterbi decoder was used for decoding. The binary-input decoder is replaced with a soft-input Viterbi decoder with a bit width of 16 bits for each of the two soft inputs (a rate 1/2 convolutional code is used). The Viterbi decoder is available as a preimplemented block in the DSP builder library. The max-log LLRs are scaled and clipped to be accommodated in 16 bits.

3. Generate inserted training symbols: For generating the inserted training symbols at the receiver, the procedure described in Papers A and B is implemented. The initial LS estimates computed from LT are used to compute the LLRs of coded bits in the first several OFDM symbols and to decode the SERVICE field which includes scrambler initialization and M'_{P}. Using the scrambler initialization, M'_{P}, and the training sequence inserted, the inserted PT symbols are generated.

4. Channel estimation: The existing implementation used the LS channel estimates computed using the LT symbols for equalizing the received symbols for the entire frame. The implementation is updated to use the generated PT symbols. The PT symbols are used to compute LS channel estimates at the PT symbol positions. These channel estimates are utilized using either the PT Hold or the PT Linear channel estimation schemes described in Paper B.

3.6 Summary

In this chapter, the 802.11p frame format and its pilot pattern were studied. A brief overview of the channel estimation schemes studied in literature for the 802.11p systems was given. The modified frame format with complementary training symbols, which is the result of the cross-layered pilot schemes proposed in the appended papers was introduced. The FER performances of some of the channel estimation schemes were compared. It was shown through simulations that the modified frames can provide good FER performance with low complexity channel estimation schemes for a suitably chosen period of pilot insertion.

With the recent developments in the graphical tools for FPGA implementation, it is possible for an algorithm developer with limited knowledge of HDLs to implement and verify algorithms on an FPGA platform. However, there exist many differences between commonly used HLL simulations for algorithm verification and FPGA implementation. In this chapter, some of the important differences were highlighted.

Chapter 4

Antenna Systems for V2V Communications

Antenna systems for V2V communications have to be designed to support the necessary ITS applications in all traffic scenarios. In contrast to cellular communications, where a base station antenna is located much higher than a user equipment and its antennas, the transmitting and receiving antennas in V2V communications are situated at similar heights. Furthermore, large metallic roofs and components of the present-day vehicles have a great influence on the directive gain patterns of the antennas mounted on the vehicles. These factors present a challenge in designing antenna systems that are well suited for V2V communications. In this chapter, an overview of the antenna systems considered for V2V communications is given.

4.1 Antenna Placement on Vehicles

A shark fin antenna module located on a vehicle's roof has been the most common method of housing antennas on vehicles. Such a module is used for housing the antennas for global navigation satellite systems, digital audio broadcast systems, cellular communications, etc. For these systems, the directive gain of the antennas in small elevation angles with respect to the roof of a vehicle is not the most important factor as the transmitted or received signals are not restricted to these small elevation angles. Therefore, the shark fin antenna module is a reasonable choice for housing the antennas for the above mentioned systems. However, in V2V communications, the transmitted and received signals are restricted to small elevation angles with respect to the roof of the vehicles due to transmitting and receiving antennas being located at similar heights. As a consequence, the directive gains of the antennas need to satisfy a minimum requirement in the entire azimuth plane to enable omnidirectional V2V communications. It may be challenging to ensure the minimum required directive gains depending on the position of the antennas

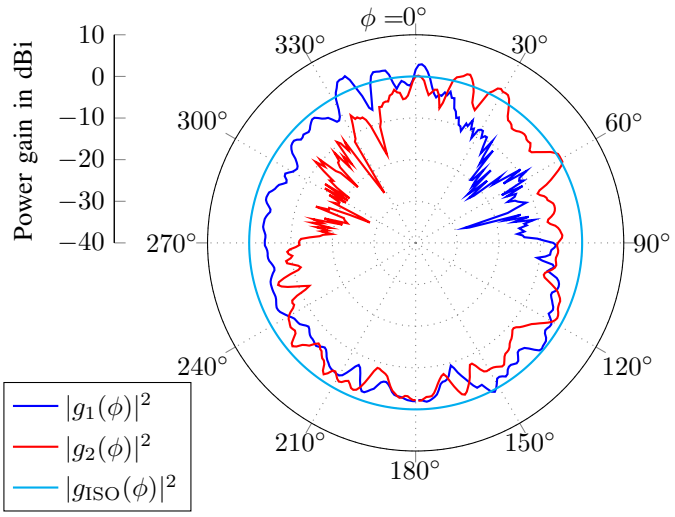

Figure 4.1: Measured directive gains of two monopole antennas placed on the roof of a Volvo XC90 in the azimuth plane. The front of the car coincides with $\phi = 0$.

in a vehicle with a metallic roof and body[1].

In [8], the measured directive gain pattern of an antenna placed on a vehicle's roof is presented. The measurements show that the directive gains in the driving direction in the azimuth plane are low due to the blocking caused by the inclined roof of the vehicle. Low gains or nulls in certain directions are undesired in vehicular scenarios, such as highway traffic, where packets arrive at the antenna with a narrow angular spread or, a dominant multipath or a LOS component [57]. Although it seems like an obvious solution to move the antenna to a position on the roof such that it experiences less blockage from the inclination of the roof, such a solution may not be feasible due to aesthetic and aerodynamics requirements of a vehicle. As a result, the most widely used shark fin antenna module normally located on the rear end of a vehicle's roof may not be the most favorable choice for housing antennas on all vehicles with varying roof inclinations. Furthermore, the effect of other factors, such as a roof luggage box, on the directive gains of roof mounted antennas have to be considered. As an example, Figure 4.1 shows the directive gains of two monopole antennas separated by a distance of 0.8 m placed on the roof of a Volvo XC90 with roof rails. The measurements were performed on the vertical polarization in the azimuth plane at a frequency of 5.9 GHz[2]. The directive gains in the direction of the roof rails are low, which implies low SNRs for packets arriving from the directions with low gains.

[1]Considering the majority of the present-day vehicles whose roof and body are metallic.

[2]Measurements were performed by Kristian Karlsson (kristian.karlsson@sp.se) and Jan Carlsson (jan.carlsson@provinn.se).

The influence of the position of an antenna, inclination of the roof, and the aesthetic considerations on the directive gains has motivated researchers and engineers to explore different solutions and locations for antennas to provide omnidirectional coverage. In [29–31], the influence of different antenna positions on V2V communications has been investigated through a simulation tool that models vehicular channels from three-dimensional environment and traffic models. Various antenna positions such as the roof, front and rear bumpers, side mirrors, and under the car have been investigated. It is concluded from the observed results that it is beneficial to use antennas mounted at different locations along with diversity combining for improved reliability against fading and to obtain omnidirectional coverage. In [32], an antenna in the shark fin module was complemented with three other antennas located at the front windscreen, side mirror, and front bumper to study the benefits of diversity and achieve omnidirectional coverage using multiple antennas. It is shown through measurements that a pair of antennas with complementary directive gains, e.g., the antenna in the shark fin module having larger gains in the backward direction and either the front windscreen or the bumper antenna with larger gains in the front direction provide omnidirectional coverage. This motivates the use of multiple antennas that are located wide apart on vehicles. However, the benefit of locating the antennas wide apart comes at the disadvantage of connecting them to the transceiver using cables with high attenuation loss or expensive digital buses.

4.2 Multiantenna Schemes for V2V Communications

Transmitter diversity, receiver diversity, and MIMO schemes that use multiple antennas for increased throughput and/or reliability is a well researched topic in wireless communications [36, 37]. However, the all-to-all broadcast nature of the CAM packets in V2V communications puts a constraint on the multiple antenna schemes that can be used. The feasibility of different multiple antenna techniques for V2V communications have to be evaluated from both transmission and reception perspectives.

The CAMs are intended for all the users in the vicinity of a transmitter, and receivers do not feedback their channel state to the transmitter. As a consequence, multiple antenna transmission techniques making use of channel state information at the transmitter (CSIT) are not feasible. Furthermore, reciprocity based CSIT acquisition is not suitable due to high mobility of the vehicles and the possibility of a large number of receivers. Hence, multiple antenna transmission for V2V broadcast communications is restricted to schemes that do not require CSIT. As a consequence, space-time block codes (STBCs) that do not require CSIT have been proposed for V2V broadcast to improve the reliability through transmit diversity [58–61]. It has been shown in [59, 60] through simulations that significant improvement in FER and BER performance can be achieved in vehicular scenarios by using STBC transmission. Despite the advantages of using STBCs to improve the reliability of V2V communications, the IEEE 802.11p standard in its current form does not support STBC transmission. Modifications and enhancements required to the 802.11p standard to support 2 transmit antenna STBC in time-varying channels have been described in detail in [60].

Receiver diversity schemes, namely, selection combining (SC), equal gain combining

(EGC), and maximal ratio combining (MRC) have been studied for vehicular communications. The performance improvements in terms of BER and/or FER obtained by using these methods in vehicular scenarios has been shown in [62–64]. In [64], the benefit of combining the output of multiple antennas using MRC in urban traffic scenarios has been shown through FER simulations. The FER performance of the combining schemes in different traffic scenarios has been compared in [62, Table II] for 2 and 4 receive antennas. The comparison in [62] aids in the selection of a suitable combination of an antenna combining scheme and number of receive antennas, where each combination has a different complexity and cost.

The receiver diversity schemes discussed above aim to improve the average SNR and/or the distribution of the instantaneous SNR and thereby increase the probability of successfully decoding every packet. The CAMs contain the information regarding the physical quantities such as direction, velocity, etc., and the information contained in the consecutive packets is highly correlated. As a result, the unsuccessful decoding of a single CAM from a vehicle may not have a serious impact on the functioning of safety applications. However, the unsuccessful decoding of several consecutive packets, i.e., a packet burst error, from the vehicle can cause a safety application to lose the current status of the vehicle, hindering the normal functioning of the application. The probability of such an event is high in the case of a single receive antenna with low directive gains in certain directions in traffic scenarios with a dominant component; where a packet burst error can occur when the consecutive packets from the vehicle arrive in the directions with low gains. Such burst errors can be prevented by using multiple antennas with contrasting directive gains and using receiver combining schemes.

In Paper C, we propose a simple antenna combining scheme to combine the output of L directional antennas to the input of a single-port receiver to minimize the probability of burst errors of K consecutive packets when packets arrive with narrow angular spreads. The combining scheme does not require measuring of instantaneous complex channel gains or SNR at the output of each antenna in contrast to the well known antenna combining schemes. This combining scheme allows the use of multiple antennas to minimize the probability of burst errors in the case of a single-port receiver when packets arrive from the worst-case AOAs. It is shown through theoretical and simulation results that burst error probability of packets arriving in the direction of low directive gains (of individual antenna elements) can be minimized using the proposed scheme.

4.3 Sector Antennas in V2V Communications

Multiple simultaneous transmissions can occur in dense vehicular networks due to the CSMA/CA based MAC scheme used for V2V broadcast, which is described in detail in Chapter 5. In a dense vehicular network, a nontransmitting vehicle can receive packets from several transmitters simultaneously due to the MAC mechanism. In such a scenario, the vehicle may not be able to decode a packet from any of the transmitting vehicles due to high interference. If the simultaneously transmitted packets arrive at the receiver from different directions, the interference in such a scenario can be reduced by using multiple sector antennas pointing in different directions that together provide omnidirectional

coverage. A detailed description and benefits of using sector antennas in the context of all-to-all broadcast in a dense network is discussed in Chapter 5.

4.4 Summary

Although a car or a vehicle seems like a large object to accommodate antennas, there exist several challenges in designing antenna systems for V2V communications due to metallic roof and components of vehicles, and the requirement to have good directive gains in the azimuth plane. In this chapter, some of the challenges involved in antenna placement and a few solutions to overcome them were described. Feasibility of different multi-antenna schemes in the context of V2V broadcast was also discussed. Finally, the benefits of using multiple antennas for diversity gain, omnidirectional coverage, and reducing interference was highlighted.

Chapter 5

Medium Access Control in V2V Communications

The absence of a central coordinator in V2V communications requires the transceivers to use a MAC scheme to coordinate among each other to transmit on the shared wireless channel. A MAC scheme called EDCA has been standardized for the IEEE 802.11p based V2V communications. The EDCA scheme is based on the CSMA/CA scheme with additional support to impose different priorities on different packet types. This chapter gives an overview of the EDCA scheme specified for IEEE 802.11p based V2V communications.

5.1 Enhanced Distributed Channel Access

The basic channel access mechanism of the IEEE 802.11 MAC known as distributed coordination function (DCF) uses the CSMA/CA protocol. The CSMA/CA protocol is described in detail in [17, Section 9.3.4]. Vehicles participating in the channel access mechanism are referred as nodes in this chapter. The basic access mechanism of the CSMA/CA scheme for unicast communications (where the transmitted packet is addressed to a single node) is summarized below.

1. A node with a packet to transmit monitors the channel and waits for the channel to be idle for a duration referred to as DCF interframe space (DIFS).

2. If the channel is found to be idle for a DIFS, it gains access to the channel and transmits a packet; otherwise, the node continues to monitor the channel.

3. When the channel is sensed idle for a DIFS, the node begins a backoff routine: the node draws an integer, referred as backoff counter (BC), uniformly from the interval $[0, 2^m W - 1]$, $m = 0$ and decrements the chosen value by one when the channel is sensed idle for a duration referred to as a slot duration. The parameter

m is referred to as the backoff stage and W is the minimum contention window size.

4. The decrement is paused if the channel is sensed busy due to another node transmitting and the decrement is resumed when the channel is sensed idle for a DIFS.

5. When the backoff value reaches zero, the node gains channel access, transmits the packet, and waits for a positive acknowledgement.

6. If a positive acknowledgment is not received within a predefined timeout interval, the transmitted packet is considered as not successfully delivered due to a possible packet collision at the receiver. The node attempts a retransmission of the packet and begins another backoff routine, this time however the node increments the backoff stage m by one and draws an integer uniformly from a larger interval $[0, 2^m W - 1]$. The backoff stage m is upper bounded by a maximum limit and the node discards the packet after a predefined number of retransmission attempts.

7. When a positive acknowledgement is received, m is reset to 0. Before transmitting a new packet, the node initiates a backoff procedure.

8. A node may be allowed to transmit multiple packets after gaining access to the channel. The duration over which the node is allowed to transmit multiple packets is indicated by transmission opportunity (TXOP). When TXOP is set to 0, a node can transmit only a single packet after gaining access to the channel.

The CSMA/CA mechanism described above requires the receivers to acknowledge the successful decoding of packets. In V2V all-to-all broadcast scenario, a packet transmitted from a vehicle is intended to all the vehicles in its transmission range. If all the receivers that successfully decode the transmitted packet were to report the success through an acknowledgment, it would require a large portion of the available time and bandwidth resources and also increase the latency between data packet transmissions. Therefore, in the broadcast mode, acknowledgments are omitted from the channel access mechanism. As a direct consequence, retransmission of packets is not supported in the broadcast scenario and the backoff procedure for a packet is only performed once (backoff stage m does not exceed 0). The absence of retransmission implies that the first and the only transmission of a packet has to be reliable. Furthermore, broadcast transmission and the absence of acknowledgments does not support the use of virtual carrier sensing mechanism that uses the request to send (RTS) and clear to send (CTS) packets to improve the channel access [17, Section 9.3].

The DCF protocol has no built-in mechanism to differentiate packets of different priorities and quality of service requirements. To allow prioritization of packets, the EDCA scheme has been specified as the MAC scheme in ITS-G5 and DSRC standards [4, 5]. The EDCA scheme is based on the DCF scheme with enhancements required to assign different priorities to packets of different types. In EDCA, packets with different priorities and quality-of-service requirements are assigned to different access classes (ACs). In contrast to the DCF scheme that requires the channel to be idle for a fixed DIFS for all packets, the EDCA requires the channel to be idle for an arbitration interframe space

Table 5.1: Mapping of different EDCA ACs to vehicular messages.

AC	Intended use	W	AIFS
AC_VO	High-priority DENM	3	58 μs
AC_VI	DENM	7	71 μs
AC_BE	CAM	15	110 μs
AC_BK	Multihop DENM, other data traffic	15	149 μs

(AIFS) that is unique for each AC. Furthermore, different contention window sizes can be assigned to each of the ACs. By assigning different AIFS and contention window sizes for different ACs, EDCA allows ACs with higher priorities to gain early and frequent access to the channel than the ACs with lower priorities. Separate medium access procedures are followed for each ACs at a node and in the case of a tie between the different ACs, an AC with higher priority is allowed to transmit a packet. Four ACs are specified for 802.11p based vehicular communications in [45, 65]. The mapping of DENM and CAM packets to the different ACs is specified in [65, Table 4-5] and is as shown in Table 5.1. As seen from the table, the messages with higher priority are assigned smaller AIFS and contention windows sizes. The names of the ACs correspond to voice (VO), video (VI), best effort (BE), and background (BK) packet traffic types for which the EDCA scheme was initially designed for. The DENM packets are event triggered and are generated occasionally in contrast to the CAM packets that are generated periodically.

The BC decrement procedure in EDCA is slightly different from the procedure in DCF. The EDCA channel access procedure is described in detail in [17, Section 9.19.2]. The BC decrement procedures in DCF and EDCA are illustrated in Figure 5.1 and Figure 5.2, respectively [35]. A node with an ongoing backoff procedure with its BC equal to 1 is chosen for the illustration. The following terminology is used in the literature to describe the backoff procedure,

- busy slot: a medium busy phase followed by a channel idle period of DIFS or AIFS;
- idle slot: a channel idle period of a slot duration after a busy slot.

The term 'generic slots' is used to refer to either of the slots. In DCF, the BC is decremented after an idle slot; whereas, the counter is decremented at the generic slot boundaries in EDCA. Furthermore, in DCF, the decrement of the counter to 0 and the transmission of a packet can both occur at the end of the same idle slot; however, in EDCA, the transmission of a packet occurs at the next slot boundary after the decrement to 0. The throughput of DCF and EDCA schemes for a scenario have been compared in [35] and it has been shown that the difference in the backoff procedures has a noticeable impact on the performance. The EDCA mechanism in the broadcast mode assuming a single AC is illustrated using a flowchart in Figure 5.3. The possibility of the packet queue being empty is also taken into consideration. The flowchart is drawn using the procedures described in [17, Section 9.19.2] and [35].

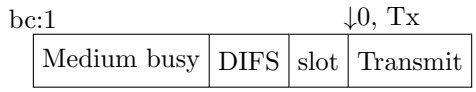

(a) Transmission after a single busy event.

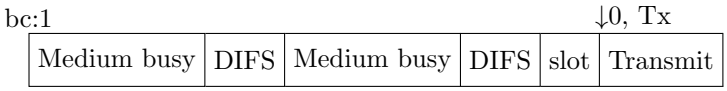

(b) Transmission after two consecutive busy events.

Figure 5.1: Illustration of BC decrement in DCF. The node waits for a slot duration after DIFS to decrement the BC and transmit.

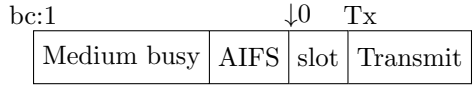

(a) Transmission after a single busy event.

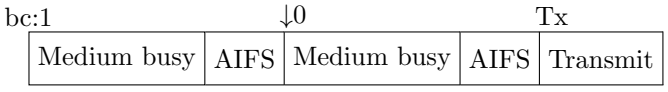

(b) Transmission after two consecutive busy events.

Figure 5.2: Illustration of BC decrement in EDCA. Note that an idle slot is not required after AIFS to decrement the BC. However, decrement of the BC and transmission cannot happen at the same event boundary.

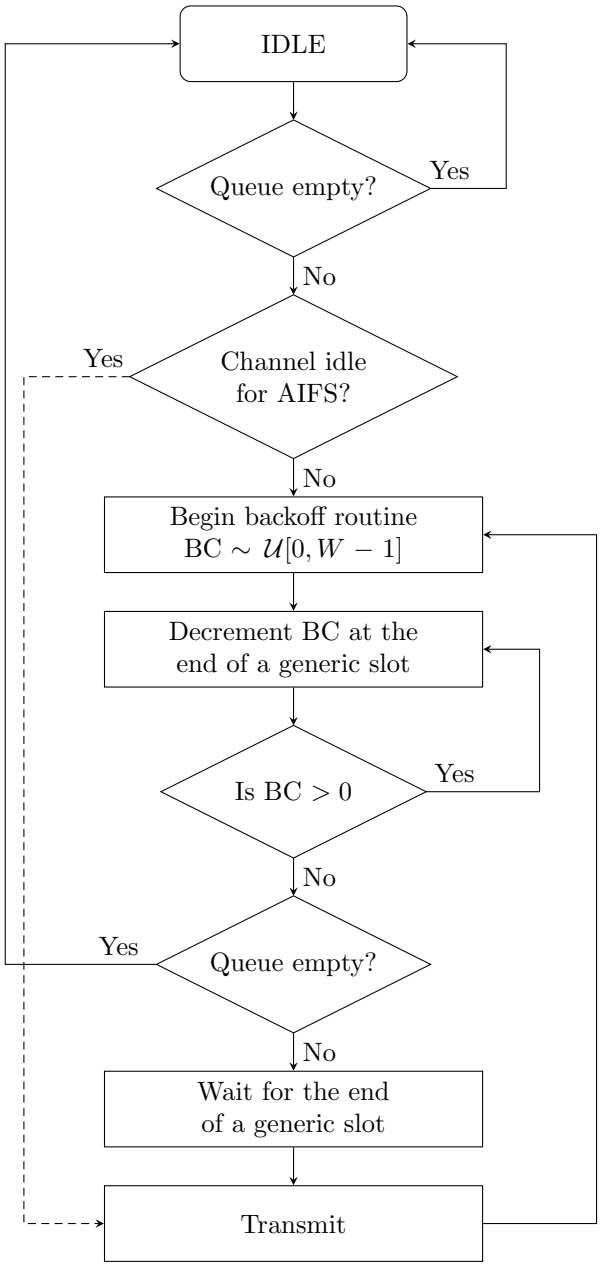

Figure 5.3: Flowchart illustrating the EDCA procedure in the broadcast mode. The randomly initialized backoff counter is denoted by BC. A generic slot refers to either a busy slot or an idle slot.

5.2 Performance Analysis of EDCA

Two main approaches have been used to study the performance of the 802.11 MAC schemes in literature. First approach consists of using discrete event simulations to simulate the network with the MAC scheme. Simulators such as NS3, OMNET++, and MATLAB have been used to simulate the networks in detail and extract the relevant performance metrics [33, 35]. In the second approach, the states of the medium access procedure at a node and transitions between the states are modeled using discrete time Markov chains (DTMCs) and the steady state probabilities are mapped to relevant performance metrics. The DTMC setup first proposed in [66] has been adopted to study the performance of different MAC schemes in the literature.

The packet arrival rate at the packet queue and the size of the queue at a transmitter has a significant impact on the performance of the MAC schemes. Based on the nature of the transmission queue, the MAC schemes have been studied in two distinct scenarios, commonly referred in the literature as the saturated and the unsaturated scenarios. In the saturated scenario, a transmitter always has a packet to transmit after the completion of a packet transmission; whereas in the unsaturated scenario, a transmitter might go into an idle state after a packet transmission due an empty transmission queue. The CAM packets in V2V communications are generated periodically at a rate of 1 to 10 Hz [6, Table 1], which could result in empty queues after a packet transmission. Therefore, the medium access for CAM packets has to be studied in the unsaturated scenario.

Different performance metrics have been considered in the literature to quantify the performance of the MAC schemes. Some important metrics discussed in the literature are listed below [33, 35, 66].

1. Utilization: Fraction of the time during which the channel is used to successfully transmit data bits. It can also be expressed as, throughput, the number of packets successfully decoded per second.

2. PSR: Fraction of the transmitted packets successfully decoded at a receiver. It is also referred to as packet reception probability in the literature.

3. Channel access delay or service time: The duration between a packet arriving at the transmitter queue and the packet being transmitted.

4. MAC-to-MAC or end-to-end delay: The duration between the arrival of a packet at the transmitter queue and its successful reception at the receiver MAC layer.

5. Packet inter arrival time: Measured between a specific transmitter-receiver pair, it is the time elapsed between two successfully decoded packets.

A combination of the performance metrics listed above is typically necessary to evaluate the pros and cons of the MAC schemes. As an example, it is beneficial to transmit on the shared channel less frequently to reduce the number of simultaneous transmissions and improve the PSR. However, this might result in very inefficient use of the channel where the channel is unoccupied for a large fraction of the time resulting in lower utilization.

The performance of the EDCA scheme, by only considering CAM transmissions, has been studied through extensive simulations in [33]. A network of vehicles on a

highway segment is simulated with realistic propagation models. Performance metrics, namely, channel access delay, PSR, MAC-to-MAC delay, and interaarrival time are used to evaluate the performance of the MAC scheme in 802.11p based V2V communications. The performance of the 802.11p EDCA scheme is also compared with self-organizing time division multiple access (STDMA) scheme which is not based on CSMA/CA. The STDMA scheme is shown to marginally outperform the EDCA scheme with CAM packets only transmissions.

The DTMC approach has been used to study the performance of the IEEE 802.11p EDCA scheme in [67]. The interactions between the different ACs is included in the modeling and the performance of each AC in terms of throughput and access delay is discussed. Exploiting the fact that the DENM packets are generated occasionally and that the CAM packets form the majority of the transmitted packets in V2V communications, the performance of the EDCA scheme has been studied by considering only the AC_BE traffic with CAMs in [34, 35]. A DTMC model is used to model the AC_BE traffic in the unsaturated scenario where the packet arrival at the transmitter queue is modeled as a Poisson arrival process with a mean arrival rate. The PSR and throughput of the scheme under CAM packet transmission are analytically derived. Furthermore, the model is validated through simulations performed using OMNET++. An intermediate result of the model in [34, 35] is the transmission probability τ, defined as the probability with which a transmitter gains access to the channel and transmits a packet at the generic slot boundaries. The transmission probability τ derived in [34, 35] is adopted in Paper D.

The vehicular networks can be dense, i.e., the number of vehicles in each others' transmission range can be very high. Urban intersection and highway scenarios are two examples of dense vehicular networks. The large number of vehicles in the intersection scenario is due to the high density of vehicles. In the highway scenario, although the vehicles are separated by larger distances, the number of vehicles in the network is large due to the larger transmission range which is a consequence of absence of buildings and high probability of LOS links [57]. A common conclusion in the studies of EDCA is that the PSR decreases rapidly with the increase in the number of transmitting vehicles beyond a limit and the generation rate of the CAM packets [35]. Figure 5.4 shows the PSR in the case of a single dipole antenna as a function of number of vehicles for different packet arrival rate, λ packets per second per node. Refer to Paper D for a detailed description of the system setup and the parameters used; the results correspond to the path loss model 1 described in the paper. It can be observed that the PSR decreases rapidly with the increase in the number of vehicles beyond a point and the increase in packet arrival rate. The degradation in performance is mainly due to the increase in the number of simultaneous transmissions which results in a decrease in the PSR. The probability of simultaneous transmissions can be reduced by lowering the transmission probability, for example by using a larger contention window size and longer AIFS. However, this results in longer channel access delays and decrease in utilization.

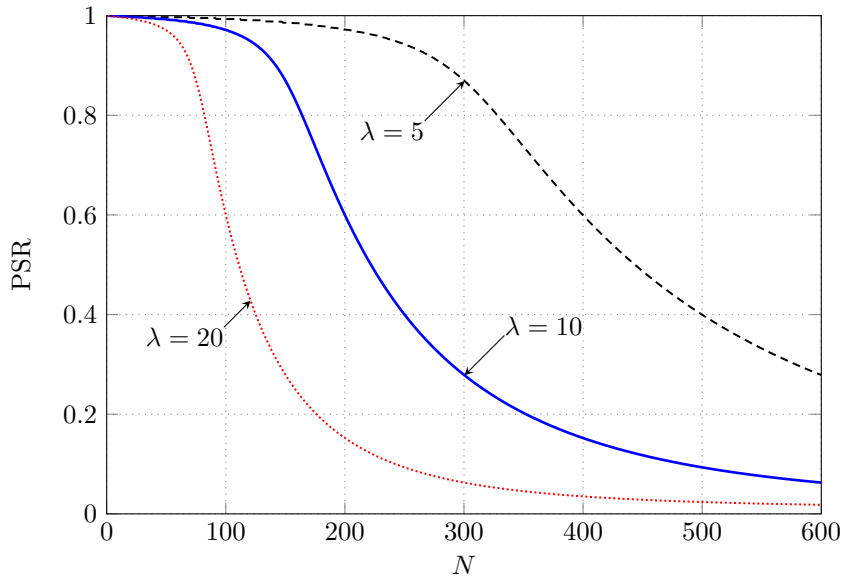

Figure 5.4: PSR for different CAM rates as a function of number of vehicles in the case of a single dipole antenna.

5.3 Sector Antennas for Dense Vehicular Scenarios

To alleviate the problem of the decrease in PSR is dense networks, solutions that exploit spatial reuse have been proposed. To reduce the number of simultaneous packets encountered by a receiver in dense networks, solutions that use sector antennas to achieve directional transmission and reception have been proposed [68–73]. The proposed solutions mainly focus on the unicast scenario, where a transmitted packet is intended to a particular receiver. The solutions advocate the use of RTS and CTS signals to inform the nodes that a transmission using a sector antenna in the direction of a receiver is planned. Using the information regarding the sector in which the transmission is planned, the other nodes can choose to not initiate a transmission in that sector or initiate a transmission in a different sector that does not interfere with the planned transmission. Variations of the idea described above are used in [68–73] to improve the PSR and throughput in dense networks with unicast transmissions. In [72, 73], schemes that use omnidirectional RTS signal, and directional CTS signals and data transmission are shown to provide significant increase in throughput and PSR.

In contrast to the unicast scenario for which the above described directional MAC schemes are proposed, the CAMs are intended for all the receivers around the transmitter. Furthermore, as mentioned in Section 5.1, the RTS and CTS signals are not supported in the broadcast mode of IEEE 802.11p. This prevents the use of the directional schemes proposed in [68–73] in IEEE 802.11p based V2V communications. However, it is

feasible to reduce the interference experienced by receivers due to multiple simultaneous transmissions in dense networks by using directional reception. By using sector antennas for reception, the interference resulting from multiple transmissions can be reduced by processing the signal arriving in the desired sector. Such a solution can be implemented in the all-to-all broadcast scenario to improve the PSR and throughput, with no modifications to the existing MAC scheme. In [74], a road side relay station at the center of a traffic intersection is equipped with sector antennas pointing in the direction of the roads. The relay station processes the received signal at each sector antenna separately to decode the packets and then relays the packets to other sectors. A collision model, where the event of two simultaneous transmissions in a sector causes the packets to be not successfully decoded, is used to analyze the PSR. It is shown through theoretical and simulation results that the PSR can be improved by several fold in dense traffic scenarios.

In Paper D, we describe a receiver setup for vehicles with sector antennas that together cover the entire azimuth. The output of each of the sector antennas is processed separately to decode a packet in the considered setup, which enables decoding of multiple packets simultaneously. A receiver in the V2V broadcast scenario is interested in decoding all the packets being transmitted, as a result it is beneficial for the receiver to decode a packet with the largest received power in the case of multiple simultaneous transmissions. Therefore, the signal-to-interference plus noise power ratio (SINR) is modeled as the largest received power divided by the sum of the remaining powers plus noise power. The decoding of the packet with the largest received power is motivated by the use of the capture effect. The capture effect means that the receiver continuously searches for a preamble with higher power even after having detected a preamble; and when a preamble with a higher power is found, it discontinues the processing of the previous packet and begins the processing of the packet with higher power [75]. To model the broadcast of CAMs based on the IEEE 802.11p EDCA scheme, we adopt the transmission probability τ derived in [34, 35]. An annular ring model is considered for distributing the vehicles, where the reference receiver is at the center of the ring and the transmitting vehicles are distributed uniformly in the annular ring. By fixing a minimum SINR threshold required to successfully decode a packet, the throughput and PSR of the network is analyzed.

Figure 5.5 shows the PSR when using the sector antenna setup described in Paper D. Refer to the paper for a detailed description of the system setup and the parameters used; the results shown in the figure are the simulated results, the theoretical bounds are omitted in this figure. The results correspond to the path loss model 1 described in the paper with a packet arrival rate of $\lambda = 10$ packets per second per node. As seen in the figure, the PSR improves dramatically in the case of both four nonoverlapping (4NO) and four partially overlapping (4OA) sector antennas in dense networks. The gain in PSR is mainly due to two factors: i) reduced interference due to sector antennas and ii) the capability of the receiver to decode upto four packets simultaneously. The drastic improvement in the PSR in the sector antenna setup comes at the expense of increased complexity and cost.

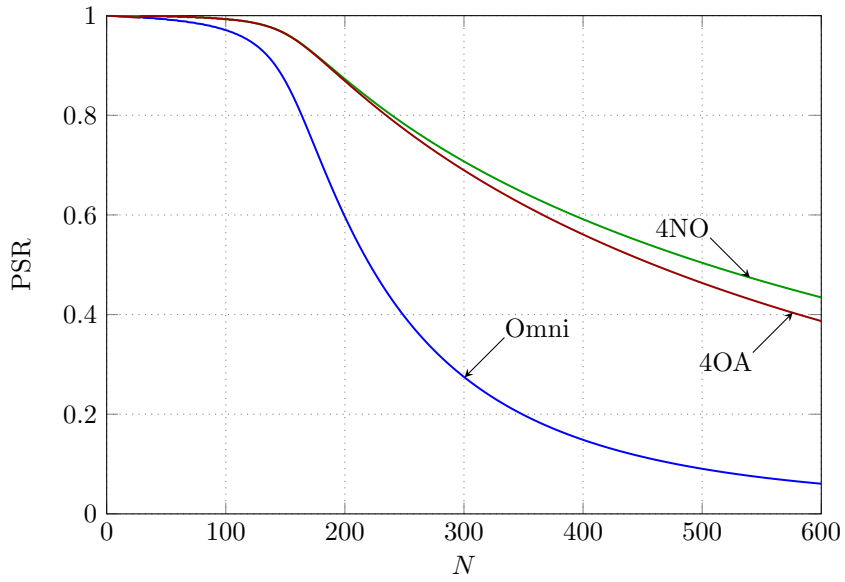

Figure 5.5: PSR for different antenna configurations for a fixed CAM rate of $\lambda = 10$ as a function on N.

5.4 Summary

An overview of the EDCA medium access scheme used in V2V communications was given in this chapter. The ability of the EDCA mechanism to impose different priorities on different packet types through ACs was discussed. The approaches used to analyze the EDCA scheme and the relevant performance metrics were briefly described. The degradation of PSR in the case of all-to-all broadcast in dense vehicular networks was highlighted. Finally, the benefits of using sector antennas with a receiver that can process the output of each antenna separately to decode packets in dense vehicular scenarios to improve the PSR was discussed.

Chapter 6

Contributions and Conclusions

6.1 Contributions

This thesis studies a few solutions to improve the robustness of V2X communications. The investigations performed in the thesis relate to:

- improving the channel estimation in 802.11p by proposing a cross-layered pilot scheme to insert complementary pilots,
- combining the output of multiple directional antennas to provide robust connectivity for packets arriving in the directions with low directivity gains in the case of a single-port receiver, and
- improving the packet success ratio in dense vehicular networks using sector antennas and a receiver that can decode multiple packets simultaneously.

The contributions made by the author are presented in Part II of the thesis in the form of four papers summarized below.

6.1.1 Paper A: "On Channel Estimation for 802.11p in Highly Time-Varying Vehicular Channels"

In Paper A, a cross-layered pilot insertion scheme to insert complementary pilots into the 802.11p frame is proposed. The proposed scheme enables the insertion of pilots above the MAC layer and hence allows a standard transmitter to transmit modified frames with the complementary pilots. A modified receiver can utilize the inserted pilots for robust channel estimation. A standard receiver sees the additional pilots as data and passes them to the higher layers, where they are removed. A modified receiver that performs robust channel estimation utilizing the inserted complementary pilots and LMMSE interpolation is described. Blockwise LMMSE interpolator that performs LMMSE interpolation in blocks is also discussed to reduce the complexity of the LMMSE interpolation. Numerical

results show that FER performance close to the case with perfect CSI is achieved with blockwise LMMSE interpolation for a suitably chosen period for pilot insertion.

6.1.2 Paper B: "An 802.11p Cross-layered Pilot Scheme for Time- and Frequency-Varying Channels and Its Hardware Implementation"

In Paper B, the procedure to insert complementary training symbols proposed in Paper A is further improved to include support for short frames. Two low-complexity channel estimation schemes that utilize the inserted pilots in modified frames for improved channel estimation are presented. The hardware implementation feasibility of the proposed scheme is shown by implementing a modified receiver in an FPGA platform. Also, the backward compatibility of the proposed scheme is verified by performing compatibility tests with a standard compliant commercial 802.11p transceiver. FER measurements are performed by interfacing the FPGA implementation with a channel emulator. FER performance of the modified receiver follows the performance of a receiver with the knowledge of perfect CSI with an offset of 3.5 to 4 dB in SNR for a suitably chosen period of pilot insertion, and the modified receiver significantly outperforms the commercial 802.11p transceiver we tested.

6.1.3 Paper C:"Robust Connectivity with Multiple Directional Antennas for Vehicular Communications"

In Paper C, a low complexity antenna combining scheme is proposed to minimize the probability of a burst of consecutive packet errors when antenna elements exhibit low gains in certain directions and the received signal power is dominated by a single component. The scheme combines the output of L directional antennas to the input of a single-port receiver using $L-1$ analog phase shifters whose phases are affine functions of time. Moreover, the scheme does not require the measurement of SNRs or complex channel gains at the output of the antennas. The proposed scheme relies on the fact that an unsuccessful decoding of K consecutive packets from a vehicle is more critical to the functioning of a safety application in comparison to the unsuccessful decoding of a single packet. It is shown using measured and simulated antenna directive gain patterns that the scheme decreases the probability of burst errors when packets arrive in directions with low gains (of individual antennas) in comparison to using one of the antennas, making the communications robust to any AOA.

6.1.4 Paper D:"Performance Analysis of Receivers using Sector Antennas for Broadcast Vehicular Communications"

In Paper D, the performance of a receiver setup with sector antennas is analyzed in the case of all-to-all broadcast communications. In the considered setup, the output of each antenna can be processed separately to decode multiple packets simultaneously. Since a receiver is interested in decoding packets from every transmitter in V2V broadcast, it is beneficial to decode a packet with the highest received power. Hence, the SINR

used to study the packet success ratio is modeled as the highest received power divided by the sum of the remaining powers plus the noise power. Furthermore, the model allows the directive gain patterns of adjacent antennas to partially overlap. The model is applied to the scenario where transmitting vehicles are uniformly distributed in an annular ring with a receiver in its center. Simulation results and theoretical bounds are used to show that a several fold increase in packet success ratio can be achieved with the sector antennas setup in dense vehicular networks in comparison to using a single omnidirectional antenna.

6.2 Conclusions and Future Work

In this thesis, specific challenges of V2X communications and the solutions proposed in the literature to overcome them were described. Since the V2X technology promises to support safety critical traffic applications, it is necessary to design a communications system that is robust to worst-case scenarios rather than optimizing for average performance. To this end, a few solutions that improve the reliability and robustness of V2V communications system were proposed and discussed in the thesis.

The IEEE 802.11p standard has not been modified to include more training symbols for aiding in channel estimation since it was specified for V2X communications. Using the pilot scheme proposed in Papers A and B, it is possible to use a standard transceiver implementing the MAC and PHY of IEEE 802.11p to insert additional training symbols in the transmitted frame. A modified transceiver can utilize the added training symbols to perform accurate channel estimation in highly time- and frequency-varying channels using low-complexity algorithms. A standard transceiver can still decode the modified frame, but will not be able to utilize the additional training symbols.

For a single-port receiver, we can use the simple analog combining network consisting of phase shifters and adders, proposed in Paper C, to combine the output of L directional antennas to improve robustness. The combining network significantly reduces the burst error probability in the worst-case angle-of-arrival compared with any one of the directional antennas. The network does not require the measurement of SNRs or channel state information. When a multiport receiver with M ports (where $1 < M < L$) that can perform MRC combining of input signals is available, a scheme that combines the output of L antennas to M signals without requiring any measurements is beneficial; this needs further investigation.

The sector antennas setup with the ability to decode multiple packets simultaneously, described in Paper D, significantly improves the packet success ratio for a system using EDCA and all-to-all broadcast in dense vehicular networks compared with the single omnidirectional antenna setup. The performance gain of the setup can be assessed analytically, which reduces the need for extensive Monte-Carlo simulations. In contrast to the antenna combining network in Paper C, the setup in Paper D is expensive due to the requirement of a receiver setup with the ability to decode multiple packets simultaneously. A simple distribution of vehicles and propagation model are considered in Paper D to evaluate the performance of the sector antenna setup. The performance gain of the setup in more realistic propagation models will be investigated in the future.

References

[1] "Intelligent transport systems (ITS); vehicular communications; basic set of applications; definitions," *ETSI TR 102 638 (V1.1.1)*, June 2009.

[2] "Car 2 Car Communication Consortium," https://www.car-2-car.org/index.php?id=171, accessed: 2018-03-06.

[3] D. Eckhoff, B. Halmos, and R. German, "Potentials and limitations of green light optimal speed advisory systems," in *Proc. IEEE Vehicular Networking Conference*, Boston, MA, USA, Dec. 2013, pp. 103–110.

[4] E. G. Ström, "On medium access and physical layer standards for cooperative intelligent transport systems in Europe," *Proceedings of the IEEE*, vol. 99, no. 7, pp. 1183–1188, July 2011, Invited paper.

[5] J. B. Kenney, "Dedicated short-range communications (DSRC) standards in the United States," *Proceedings of the IEEE*, vol. 99, no. 7, pp. 1162–1182, July 2011, Invited paper.

[6] "Intelligent transport systems (ITS); vehicular communications; basic set of applications; part 2: Specification of cooperative awareness basic service," *ETSI TS 102 637-2 (V1.2.1)*, Mar. 2011.

[7] "Intelligent transport systems (ITS); vehicular communications; basic set of applications; part 3: Specifications of decentralized environmental notification basic service," *ETSI TS 102 637-3 (V1.1.1)*, Sep. 2010.

[8] C. Mecklenbräuker, A. F. Molisch, J. Karedal, F. Tufvesson, A. Paier, L. Bernadó, T. Zemen, O. Klemp, and N. Czink, "Vehicular channel characterization and its implications for wireless system design and performance," *Proceedings of the IEEE*, vol. 99, no. 7, pp. 1189–1212, July 2011.

[9] G. Acosta-Marum and M. Ingram, "Doubly selective vehicle-to-vehicle channel measurements and modeling at 5.9 GHz," in *Proc. International Symposium on Wireless Personal Multimedia Communications*, San Diego, CA, USA, 2006.

[10] D. Matolak, I. Sen, and W. Xiong, "Channel modeling for V2V communications," in *Proc. Third Annual International Conference on Mobile and Ubiquitous Systems: Networking Services*, San Jose, CA, USA, July 2006, pp. 1–7.

[11] G. Acosta-Marum and M. Ingram, "Six time- and frequency-selective empirical channel models for vehicular wireless LANs," *IEEE Vehicular Technology Magazine*, vol. 2, no. 4, pp. 4–11, Dec. 2007.

[12] I. Sen and D. Matolak, "Vehicle-vehicle channel models for the 5-GHz band," *IEEE Transactions on Intelligent Transportation Systems*, vol. 9, no. 2, pp. 235–245, June 2008.

[13] A. Paier, "The vehicular radio channel in the 5 GHz band," Ph.D. dissertation, Institut für Nachrichtentechnik und Hochfrequenztechnik (E389), Vienna University of Technology, Oct. 2010.

[14] L. Bernadó, T. Zemen, F. Tufvesson, A. F. Molisch, and C. Mecklenbräuker, "Delay and Doppler spreads of nonstationary vehicular channels for safety-relevant scenarios," *IEEE Transactions on Vehicular Technology*, vol. 63, no. 1, pp. 82–93, Jan. 2014.

[15] T. Abbas, "Measurement based channel characterization and modeling for vehicle-to-vehicle communications," Ph.D. dissertation, Department of Electrical and Information Technology, Lund University, Jan. 2014.

[16] "Wireless LAN medium access control (MAC) and physical layer (PHY) specifications, Amendment 6: Wireless access in vehicular environments," *IEEE Std 802.11p-2010*, pp. 1–51, 2010.

[17] "Wireless LAN medium access control (MAC) and physical layer (PHY) specifications," *IEEE Std 802.11-2012*, pp. 1–2793, 2012.

[18] R. Grünheid, H. Rohling, J. Ran, E. Bolinth, and R. Kern, "Robust channel estimation in wireless LANs for mobile environments," in *Proc. IEEE Vehicular Technology Conference*, Vancouver, BC, Canada, Sept. 2002, pp. 1545–1549.

[19] W. Cho, S. I. Kim, H.-K. Choi, H.-S. Oh, and D.-Y. Kwak, "Performance evaluation of V2V/V2I communications: The effect of midamble insertion," in *Proc. 1st International Conference on Wireless Communication, Vehicular Technology, Information Theory and Aerospace Electronic Systems Technology*, Aalborg, Denmark, May 2009, pp. 793–797.

[20] S. Sibecas, C. Corral, S. Emami, G. Stratis, and G. Rasor, "Pseudo-pilot OFDM scheme for 802.11a and R/A in DSRC applications," in *Proc. IEEE Vehicular Technology Conference*, Orlando, FL, USA, Oct. 2003, pp. 1234–1237.

[21] T. Kella, "Decision-directed channel estimation for supporting higher terminal velocities in OFDM based WLANs," in *Proc. IEEE Global Telecommunications Conference*, San Francisco, CA, USA, Dec. 2003, pp. 1306–1310.

[22] J. Fernandez, D. Stancil, and F. Bai, "Dynamic channel equalization for IEEE 802.11p waveforms in the vehicle-to-vehicle channel," in *Proc. Allerton Conference on Communication, Control, and Computing*, Allerton, IL, USA, Sept. 2010, pp. 542–551.

[23] J. Fernandez, K. Borries, L. Cheng, B. Kumar, D. Stancil, and F. Bai, "Performance of the 802.11p physical layer in vehicle-to-vehicle environments," *IEEE Transactions on Vehicular Technology*, vol. 61, no. 1, pp. 3–14, Jan. 2012.

[24] Z. Zhao, X. Cheng, M. Wen, B. Jiao, and C.-X. Wang, "Channel estimation schemes for IEEE 802.11p standard," *IEEE Intelligent Transportation Systems Magazine*, vol. 5, no. 4, pp. 38–49, Oct. 2013.

[25] Z. Zhao, X. Cheng, M. Wen, L. Yang, and B. Jiao, "Constructed data pilot-assisted channel estimators for mobile environments," *IEEE Transactions on Intelligent Transportation Systems*, vol. 16, no. 2, pp. 947–957, Apr. 2015.

[26] T. Zemen, L. Bernadó, N. Czink, and A. F. Molisch, "Iterative time-variant channel estimation for 802.11p using generalized discrete prolate spheroidal sequences," *IEEE Transactions on Vehicular Technology*, vol. 61, no. 3, pp. 1222–1233, Mar. 2012.

[27] P. Alexander, D. Haley, and A. Grant, "Cooperative intelligent transport systems: 5.9-GHz field trials," *Proceedings of the IEEE*, vol. 99, no. 7, pp. 1213–1235, July 2011.

[28] O. Goubet, G. Baudic, F. Gabry, and T. J. Oechtering, "Low-complexity scalable iterative algorithms for IEEE 802.11p receivers," *IEEE Transactions on Vehicular Technology*, vol. 64, no. 9, pp. 3944–3956, Sept. 2015.

[29] L. Reichardt, T. Fugen, and T. Zwick, "Influence of antennas placement on car to car communications channel," in *Proc. European Conference on Antennas and Propagation*, Berlin, Germany, Mar. 2009, pp. 630–634.

[30] L. Reichardt, C. Sturm, and T. Zwick, "Performance evaluation of SISO, SIMO and MIMO antenna systems for car-to-car communications in urban environments," in *Proc. International Conference on Intelligent Transport Systems Telecommunications*, Lille, France, Oct. 2009, pp. 51–56.

[31] L. Reichardt, J. Maurer, T. Fügen, and T. Zwick, "Virtual drive: A complete V2X communication and radar system simulator for optimization of multiple antenna systems," *Proceedings of the IEEE*, vol. 99, no. 7, pp. 1295–1310, July 2011.

[32] T. Abbas, J. Karedal, and F. Tufvesson, "Measurement-based analysis: The effect of complementary antennas and diversity on vehicle-to-vehicle communication," *IEEE Antennas and Wireless Propagation Letters*, vol. 12, pp. 309–312, Mar. 2013.

[33] K. Sjöberg, "Medium access control for vehicular ad hoc networks," Ph.D. dissertation, School of Information Science, Computer and Electrical Engineering, Halmstad University, Apr. 2013.

[34] G. Heijenk, M. van Eenennaam, and A. Remke, "Performance comparison of IEEE 802.11 DCF and EDCA for beaconing in vehicular networks," in *International Conference on Quantitative Evaluation of Systems*. Springer, 2014, pp. 154–169.

[35] M. van Eenennaam, "Scalable beaconing for cooperative adaptive cruise control," Ph.D. dissertation, University of Twente, Netherlands, Nov. 2013.

[36] A. Goldsmith, *Wireless communications*. Cambridge University Press, 2005.

[37] A. F. Molisch, *Wireless communications*. John Wiley & Sons, 2007.

[38] D. Tse and P. Viswanath, *Fundamentals of Wireless Communication.* Cambridge University Press, 2005.

[39] J. Kunisch and J. Pamp, "Wideband car-to-car radio channel measurements and model at 5.9 GHz," in *Proc. IEEE Vehicular Technology Conference*, Calgary, BC, Canada, Sept. 2008, pp. 1–5.

[40] J. Karedal, N. Czink, A. Paier, F. Tufvesson, and A. Molisch, "Path loss modeling for vehicle-to-vehicle communications," *IEEE Transactions on Vehicular Technology*, vol. 60, no. 1, pp. 323–328, Jan. 2011.

[41] G. Matz, "On non-WSSUS wireless fading channels," *IEEE Transactions on Wireless Communications*, vol. 4, no. 5, pp. 2465–2478, 2005.

[42] "Car-2-car communication consortium task force antannae and wireless performance-whitepaper (ver 1.2)." Tech. Rep., Oct. 2014.

[43] J. Karedal, F. Tufvesson, N. Czink, A. Paier, C. Dumard, T. Zemen, C. Mecklenbräuker, and A. Molisch, "A geometry-based stochastic MIMO model for vehicle-to-vehicle communications," *IEEE Transactions on Wireless Communications*, vol. 8, no. 7, pp. 3646–3657, July 2009.

[44] A. Molisch, "A generic model for MIMO wireless propagation channels in macro- and microcells," *IEEE Transactions on Signal Processing*, vol. 52, no. 1, pp. 61–71, Jan. 2004.

[45] "Intelligent transport systems (ITS); access layer specification for intelligent transport systems operating in the 5 GHz frequency band," *ETSI EN 302 663 (V1.2.1)*, July 2013.

[46] Y. Li and G. L. Stuber, *Orthogonal Frequency Division Multiplexing for Wireless Communications.* Springer Science & Business Media, 2006.

[47] U. Madhow, *Fundamentals of Digital Communication.* Cambridge University Press, 2008.

[48] P. Hoeher, S. Kaiser, and P. Robertson, "Two-dimensional pilot-symbol-aided channel estimation by Wiener filtering," in *Proc. IEEE International Conference on Acoustics, Speech, and Signal Processing*, Munich, Germany, Apr. 1997, pp. 1845–1848.

[49] J.-J. van de Beek, O. Edfors, M. Sandell, S. K. Wilson, and P. O. Börjesson, "On channel estimation in OFDM systems," in *Proc. IEEE Vehicular Technology Conference*, vol. 2, Chicago, IL, USA, July 1995, pp. 815–819.

[50] O. Edfors, "Low-complexity algorithms in digital receivers," Ph.D. dissertation, Luleå Tekniska Universitet, 1996.

[51] M. Sandell, "Design and analysis of estimators for multicarrier modulation and ultrasonic imaging," Ph.D. dissertation, Luleå Tekniska Universitet, 1996.

[52] O. Edfors, M. Sandell, J.-J. van de Beek, S. K. Wilson, and P. O. Börjesson, "OFDM channel estimation by singular value decomposition," in *Proc. IEEE Vehicular Technology Conference*, Atlanta, GA, USA, Apr. 1996, pp. 923–927.

[53] Y. Li, "Pilot-symbol-aided channel estimation for OFDM in wireless systems," *IEEE Transactions on Vehicular Technology*, vol. 49, no. 4, pp. 1207–1215, July 2000.

[54] H. Minn and V. Bhargava, "An investigation into time-domain approach for OFDM channel estimation," *IEEE Transactions on Broadcasting*, vol. 46, no. 4, pp. 240–248, Dec. 2000.

[55] C. Douillard, M. Jézéquel, C. Berrou, A. Picart, P. Didier, and A. Glavieux, "Iterative correction of intersymbol interference: Turbo-equalization," *European Transactions on Telecommunications*, vol. 6, no. 5, pp. 507–511, 1995.

[56] "High performance digital radio testbed (HIRATE)," http://www.hhi.fraunhofer.de/departments/wireless-communications-and-networks/research-areas/enabling-technologies-for-future-wireless-applications/hirate-high-performance-digital-radio-testbed.html, Accessed: 2015-09-23.

[57] T. Abbas, K. Sjöberg, J. Karedal, and F. Tufvesson, "A measurement based shadow fading model for vehicle-to-vehicle network simulations," *International Journal of Antennas and Propagation*, vol. 2015, May 2015.

[58] K. Ito, N. Itoh, K. Sanda, and Y. Karasawa, "A novel MIMO-STBC scheme for inter-vehicle communications at intersection," in *Proc. IEEE Vehicular Technology Conference*, vol. 6, Melbourne, Vic., Australia, May 2006, pp. 2937–2941.

[59] N. F. Abdullah, A. Doufexi, and R. J. Piechocki, "Spatial diversity for IEEE 802.11p post-crash message dissemination in a highway environment," in *Proc. IEEE Vehicular Technology Conference*, Taipei, Taiwan, May 2010, pp. 1–5.

[60] T. Mata, K. Naito, P. Boonsrimuang, K. Mori, and H. Kobayashi, "Proposal of STBC MIMO-OFDM for ITS systems," in *Proc. International Conference on Electrical Engineering/Electronics, Computer, Telecommunications and Information Technology*, Krabi, Thailand, May 2013, pp. 1–6.

[61] S. Moser, L. Behrendt, and F. Slomka, "MIMO-enabling PHY layer enhancement for vehicular ad-hoc networks," in *Proc. IEEE Wireless Communications and Networking Conference Workshops*, New Orleans, LA, USA, March 2015, pp. 142–147.

[62] J. Nuckelt, H. Hoffmann, M. Schack, and T. Kürner, "Linear diversity combining techniques employed in car-to-X communication systems," in *Proc. IEEE Vehicular Technology Conference (VTC Spring)*, Yokohama, Japan, May 2011, pp. 1–5.

[63] G. Maier, A. Paier, and C. F. Mecklenbräuker, "Performance evaluation of IEEE 802.11p infrastructure-to-vehicle real-world measurements with receive diversity," in *Proc. International Wireless Communications and Mobile Computing Conference*, Limassol, Cyprus, Aug 2012, pp. 1113–1118.

[64] J. Nuckelt and T. Kürner, "MRC performance benefit in V2V communication systems in urban traffic scenarios," in *Proc. European Conference on Antennas and Propagation (EUCAP)*, Prague, Czech Republic, Mar. 2012, pp. 2311–2315.

[65] "Intelligent transport systems (ITS); vehicular communications; geonetworking; part 4: Geographical addressing and forwarding for point-to-point and point-to-multipoint communications; sub-part 2: Media-dependent functionalities for ITS-G5," *ETSI TS 102 636-4-2 (V1.1.1)*, Oct. 2013.

[66] G. Bianchi, "Performance analysis of the IEEE 802.11 distributed coordination function," *IEEE Journal on Selected Areas in Communications*, vol. 18, no. 3, pp. 535–547, Mar. 2000.

[67] J. R. Gallardo, D. Makrakis, and H. T. Mouftah, "Performance analysis of the EDCA medium access mechanism over the control channel of an IEEE 802.11p WAVE vehicular network," in *Proc. IEEE International Conference on Communications*, Dresden, Germany, June 2009, pp. 1–6.

[68] A. Nasipuri, S. Ye, J. You, and R. E. Hiromoto, "A MAC protocol for mobile ad hoc networks using directional antennas," in *Proc. IEEE Wireless Communications and Networking Confernce*, vol. 3, Chicago, IL, USA, Sep. 2000, pp. 1214–1219.

[69] Y.-B. Ko, V. Shankarkumar, and N. H. Vaidya, "Medium access control protocols using directional antennas in ad hoc networks," in *Proc. Nineteenth Annual Joint Conference of the IEEE Computer and Communications Societies*, vol. 1, Tel Aviv, Israel, Mar. 2000, pp. 13–21.

[70] R. M. Yadumurthy, A. Chimalakonda, M. Sadashivaiah, and R. Makanaboyina, "Reliable MAC broadcast protocol in directional and omni-directional transmissions for vehicular ad hoc networks," in *Proc. the 2nd ACM International Workshop on Vehicular Ad Hoc Networks*, Cologne, Germany, Sep. 2005, pp. 10–19.

[71] R. Ramanathan, J. Redi, C. Santivanez, D. Wiggins, and S. Polit, "Ad hoc networking with directional antennas: a complete system solution," *IEEE Journal on Selected Areas in Communications*, vol. 23, no. 3, pp. 496–506, Mar. 2005.

[72] X. Xie, F. Wang, K. Li, P. Zhang, and H. Wang, "Improvement of multi-channel MAC protocol for dense VANET with directional antennas," in *Proc. IEEE Wireless Communications and Networking Conference*, Budapest, Hungary, Apr. 2009.

[73] K. Xu, B. T. Garrison, and K. C. Wang, "Performance modeling for IEEE 802.11 vehicle-to-infrastructure networks with directional antennas," in *Proc. IEEE Vehicular Networking Conference*, Jersey City, NJ, USA, Dec. 2010, pp. 215–222.

[74] H. Cheng and Y. Yamao, "Reliable inter-vehicle broadcast communication with sectorized roadside relay station," in *Proc. IEEE Vehicular Technology Conference (VTC Spring)*, Dresden, Germany, June 2013, pp. 1–5.

[75] J. Lee, W. Kim, S.-J. Lee, D. Jo, J. Ryu, T. Kwon, and Y. Choi, "An experimental study on the capture effect in 802.11a networks," in *Proc. ACM International Workshop on Wireless Network Testbeds, Experimental Evaluation and Characterization*, Montreal, Quebec, Canada, Sep. 2007, pp. 19–26.